ALINE DE CASTRO DA SILVA

NANOPARTÍCULAS HÍBRIDAS DE ÓXIDO DE FERRO E PRATA PREJUDICAM O SISTEMA COLINÉRGICO E CAUSAM REPROTOXICIDADE EM *Caenorhabditis elegans*

DISSERTAÇÃO DE MESTRADO

URUGUAIANA

2023

ALINE DE CASTRO DA SILVA

NANOPARTÍCULAS HÍBRIDAS DE ÓXIDO DE FERRO E PRATA PREJUDICAM O SISTEMA COLINÉRGICO E CAUSAM REPROTOXICIDADE EM Caenorhabditis elegans

Dissertação apresentada ao Programa de Pós-Graduação em Bioquímica da Universidade Federal do Pampa, como requisito parcial para obtenção do Título de Mestre.

Orientador(a): Daiana Silva de Ávila

URUGUAIANA

2023

Ficha catalográfica elaborada automaticamente com os dados fornecidos
pelo(a) autor(a) através do Módulo de Biblioteca do
Sistema GURI (Gestão Unificada de Recursos Institucionais) .

S586n Silva, Aline Castro
Nanopartículas Híbridas de Óxido de Ferro e Prata Impactam o Sistema Colinérgico e Causam Reprotoxicidade em Caenorhabditis elegans / Aline Castro Silva.
57 p.

Dissertação(Mestrado)-- Universidade Federal do Pampa, MESTRADO EM BIOQUÍMICA, 2023.
"Orientação: Daiana Silva Ávila".

1. nanotoxicologia. 2. NPs metálicas. 3. nanoparticulas híbridas. 4. reprodução. I. Título.

ALINE DE CASTRO DA SILVA

NANOPARTÍCULAS HÍBRIDAS DE ÓXIDO DE FERRO E PRATA PREJUDICAM O SISTEMA COLINÉRGICO E CAUSAM REPROTOXICIDADE EM *Caenorhabditis elegans*

Dissertação/Tese apresentada ao Programa de Pós-Graduação em Bioquímica da Universidade Federal do Pampa, como requisito parcial para obtenção do Título de Mestre/Doutor em Bioquímica.

Dissertação defendida e aprovada em: 21, julho e 2023.

Banca examinadora:

Profa. Dra. Daiana Silva de Ávila
Orientadora
UNIPAMPA

Prof. Dr. José Maria Monserrat
FURG

Profa. Dra. Suzan Gonçalves da Rosa
UNIPAMPA

Assinado eletronicamente por **DAIANA SILVA DE AVILA**, **PROFESSOR DO MAGISTERIO SUPERIOR**, em 31/07/2023, às 10:32, conforme horário oficial de Brasília, de acordo com as normativas legais aplicáveis.

Assinado eletronicamente por **SUZAN GONCALVES ROSA**, **PROFESSOR DO MAGISTERIO SUPERIOR**, em 31/07/2023, às 10:51, conforme horário oficial de Brasília, de acordo com as normativas legais aplicáveis.

A autenticidade deste documento pode ser conferida no site https://sei.unipampa.edu.br/sei/controlador_externo.php?acao=documento_conferir&id_orgao_acesso_externo=0, informando o código verificador **1199988** e o código CRC **9D9C339C**.

AGRADECIMENTOS

Agradeço a Deus por me dar força para continuar, com saúde, estudando em uma universidade pública e de qualidade, rodeada de pessoas que me instigam a ser melhor dia a dia.

Aos meus pais Sirlei e Luis, eu poderia escrever muitas páginas de agradecimento e ainda assim não seria suficiente. Tudo que eu sou e o que serei, vem do amor que vocês dedicaram a mim durante meus 25 anos. Obrigada por acreditarem e não medirem esforços para que eu realize meus sonhos.

Ao meu irmão, saber que tenho alguém com quem contar me da forças para seguir em busca dos meu sonhos, obrigada por existir.

A Julia, obrigada pelos 7 anos de companheirismo. Tu faz parte das minhas conquistas e independente de onde nós duas estivermos, as lembranças que construimos nesses anos estarão sempre no meu coração.

A Olivia e a Amora, minhas filhas de quatro patas, obrigada por estarem ao meu lado durante esse período, enchendo minha vida de amor para seguir em frente.

Ao Eduardo Fagundes, por me acompanhar ao longo desses anos, me dando força para que eu nunca esqueça que sou capaz e vou alcançar meus objetivos.

Aos meus amigos e colegas de pesquisa, o dia a dia no laborarório é mais leve e feliz com a presença de vocês. As conversas, festas e o conhecimento compartilhado nos torna um grupo unido e capaz de enfrentar os mais diversos desafios que a ciência nos apresenta.

A professora Daiana, saiba que tem minha admiração, é gratificante trabalhar com alguém tão competente e que valoriza seus alunos. Obrigada por acreditar no meu potencial e me dar tantas oportunidades para crescer como pessoa e profissional. Espero que continuemos a trabalhar juntas e que eu possa aprender a ser uma grande cientista como tu és.

“Ao meu passado, eu devo meu saber e a minha ignorância"

Simone de Beauvoir

RESUMO

As nanopartículas de óxido de ferro (Fe_3O_4-NPs) apresentam propriedades superparamagnéticas que possibilitam sua aplicação em diversas áreas, inclusive na liberação de fármacos em locais específicos do organismo. Já as nanopartículas de prata (Ag-NPs) têm potentes efeitos antimicrobianos. Embora a combinação de Fe_3O_4-NPs e Ag-NPs em uma nanoestrutura híbrida (Fe_3O_4@Ag-NPs) tenha demonstrado aplicações biomédicas promissoras, seus efeitos toxicológicos são desconhecidos e precisam ser melhor avaliados. Utilizamos *Caenorhabditis elegans*, um modelo estabelecido para análises nanotoxicológicas pois permite uma triagem inicial de novas substâncias. Após exposição aguda (30 minutos) de animais no primeiro estágio larval a Fe_3O_4-NPs, Ag-NPs e Fe_3O_4@Ag-NPs, observamos que as NPs híbridas reduziram a sobrevivência e reprodução de *C. elegans*. Também observamos que Fe_3O_4@Ag-NPs causaram um aumento na apoptose celular na linha germinativa e uma diminuição na postura de ovos, o que foi associado a uma diminuição nos movimentos de natação do verme e a anormalidades nos neurônios colinérgicos. Fe_3O_4@Ag-NPs causaram um aumento nos níveis de espécies reativas de oxigênio, juntamente com a ativação do fator de transcrição DAF-16. Foi evidenciada maior expressão dos genes-alvo GST-4::GFP e SOD-3::GFP, o que sugere a ativação do sistema antioxidante. Nossos resultados indicam a reprotoxicidade causada por altos níveis de Fe_3O_4@Ag-NPs, bem como neurotoxicidade colinérgica e ativação do sistema oxidante em *C. elegans*, sugerindo que altos níveis desses nanomateriais podem ser prejudiciais aos organismos vivos.

Palavras-chave: nanotoxicologia; NPs metálicas; nanopartículas híbridas; reprodução

ABSTRACT

Iron oxide nanoparticles (Fe_3O_4-NPs) exhibit superparamagnetic properties that enable their application in various areas, including drug delivery at specific locations in an organism. Silver nanoparticles (Ag-NPs) have potent antimicrobial effects. Although the combination of Fe_3O_4-NPs and Ag-NPs in one hybrid nanostructure (Fe_3O_4@Ag-NPs) demonstrated promising targeted biomedical applications, its toxicological effects are unknown and require further evaluation. We used *Caenorhabditis elegans*, an estabilished model for nanotoxicological analysis, because it allows for the initial screening of new substances. After acute exposure to Fe_3O_4-NPs, Ag-NPs, and Fe_3O_4@Ag-NPs, we observed that the hybrid NPs reduced *C. elegans* survival and reproduction. We also observed that Fe_3O_4@Ag-NPs caused an increase in germline cells apoptosis and a decrease in egg laying, which was associated with a decrease in worm swimming movements and abnormalities in cholinergic neurons. Fe_3O_4@Ag-NPs caused an increase in reactive oxygen species levels, along with the activation of the DAF-16 transcription factor. Higher expression of the target genes GST-4::GFP and SOD-3::GFP was observed, suggesting activation of the antioxidant system. Our results indicate reprotoxicity caused by high levels of Fe_3O_4@Ag-NPs, as well as cholinergic neurotoxicity and activation of the oxidant system in *C. elegans*, suggesting that high levels of these nanomaterials can be harmful to living organisms.

Keywords: nanotoxicology; metal NPs; hybrid nanoparticles; reproduction

LISTA DE FIGURAS

LISTA DE ABREVIATURAS

NPs - Nanopartículas
RM - Ressonância magnética
EROs - Espécies reativas de oxigênio
NGM - Nematode growth medium
MNPs - Nanopartículas magnéticas
OCDE - Cooperação e Desenvolvimento Econômico
nm - Nanômetros
GST-4 - Glutationa-S-transferase 4
DP- Desvio padrão
ADN - Ácido desoxirribonucleiro
HSNs- neurônios serotoninérgicos
VCs- neurônios colinérgicos ventrais C
IGFR - Receptor transmembrana de insulina
PI3K - Fosfoinositídeo 3-quinase
SOD-3 - Superóxido dismutase 3
CAT- catalase
GPX – Glutationa peroxidade
ARNm - Ácido ribobucleico mensageiro

SUMÁRIO

1. INTRODUÇÃO

A nanotecnologia vem se tornando um campo crescente de pesquisa, visto que os produtos obtidos por esse meio apresentam vantagens frente a outros produtos de mesma composição (ARRUEBO *et al.*, 2007). Estas vantagens se devem principalmente por suas propriedades relacionadas ao pequeno tamanho, à maior superfície de contato e às propriedades magnéticas e eletrônicas, que proporcionam um avanço de sua utilização em grandes áreas como o setor ambiental e biomédico (SAIFI; KHURANA; GODUGU, 2018; WU *et al.*, 2019). As NPs metálicas consistem em um metal ou núcleo de óxido metálico, encapsulado em um revestimento inorgânico ou polimérico. Suas propriedades magnéticas tornam-as de grande interesse na área biomédica por serem biocompatíveis, estáveis, podendo servir como suporte para biomoléculas (ARRUEBO *et al.*, 2007; BOEY; HO, 2020).

Estudos apontam que nanomateriais híbridos (mais de um metal) podem apresentar avanços promissores em relação às NPs monofuncionais, pois possibilita a associação de características e funções em uma única estrutura, proporcionando um progresso para aplicações de nanomateriais com propriedades específicas (PIERETTI *et al.*, 2019). Sabe-se que NPs metálicas de Fe_3O_4 e Ag apresentam aplicações biomédicas como atividade antimicrobiana (DURÁN *et al.*, 2018), antitumoral e carreadora de fármacos (GHAZANFARI *et al.*, 2016). No entanto, são poucos estudos que abordam os efeitos de nanopartículas híbridas de Fe_3O_4@Ag e, além disso, os dados existentes abordam Fe_3O_4@Ag-NPs produzidas de forma química utilizando solventes, e não através de síntese biogênica, que pode ser realizada através do uso de bactérias, fungos, extrato de plantas ou algas (PIERETTI *et al.*, 2019).

Com o aumento da aplicação de nanotecnologia na realidade atual, são necessários maiores estudos sobre a biosegurança destes materiais. Considerando a problemática da avaliação toxicológica em mamíferos e a relevância da política dos 3R's (do inglês *refine, replace, reduce*) na pesquisa

in vivo, utilizamos o *Caenorhabditis elegans,* um pequeno nematoide de vida livre amplamente encontrado em matéria orgânica em decomposição (WU *et al.*, 2019). Esse modelo experimental possui inúmeras vantagens, dentre elas, trata-se de um animal transparente, com genoma totalmente sequenciado, de fácil manipulação e manutenção (TEJEDA-BENITEZ; OLIVERO-VERBEL, 2016). O verme tem um ciclo de vida curto, que facilita a análise de parâmetros reprodutivos como o tamanho da progênie e postura de ovos. Aproximadamente 60-80% dos genes humanos têm um ortólogo no genoma de *C. elegans* e 40% dos genes conhecidos por estarem associados a doenças humanas têm ortólogos claros no genoma do *C. elegans* o que o torna um excelente modelo a nível genético (CULETTO, 2000; KALETTA; HENGARTNER, 2006). Por ser transparente, o verme pode ser estudado em detalhes através da marcação de proteínas e compartimentos celulares utilizando fluorescência. As proteínas fluorescentes também podem ser usadas para estudar processos de desenvolvimento, rastrear mutantes e função celular, isolar células e caracterizar interações de proteínas *in vivo* (CORSI, Ann K.; WIGHTMAN; CHALFIE, 2015). Dessa forma, o *C. elegans* tornou-se uma ótima ferramenta para estudos nanotoxicológicos, possibilitando avaliar os impactos destes produtos em quatro sistemas, incluindo o sistema nervoso, digestivo, imunológico e reprodutivo, o que permite que os resultados de *C. elegans* sejam confiáveis e contribuam para avanços na saúde humana (HUNT, 2017; WU *et al.*, 2019).

Neste estudo, investigamos os efeitos de tóxicos Fe_3O_4@Ag-NPs biogenicamente sintetizados usando o modelo *in vivo* de *C. elegans*. Elucidamos a ação de NPs híbridas no sistema reprodutivo, neuronal e também no sistema antioxidante, avaliando os níveis de espécies reativas de oxigênio juntamente com a modulação de DAF-16, relacionada a resposta ao estresse.

2. JUSTIFICATIVA

Individualmente, NPs de Fe_3O_4 e Ag apresentam diversas aplicações biomédicas já documentadas, dentre elas, propriedades antitumorais e antimicrobianas. Nanopartículas híbridas de Fe_3O_4@Ag vem apresentando um promissor avanço devido a possibilidade de combinar as diferentes características e funções desses nanomaterais para obtenção de um produto final com propriedades específicas.

Os estudos visando a avaliação da segurança de Fe_3O_4@Ag-NPs devem ser ampliados, uma vez que, ainda existem poucos resultados *in vivo* sobre a exposição a essas nanopartículas. Além disso, a maioria os dados existentes se concentra na toxicidade das nanopartículas de forma química, existindo poucos relatos de estudos que caracterizam a nanotoxicidade através de uma síntese biogênica.

Dessa forma, a avaliação toxicológica em um modelo experimental alternativo como o *Caenorhabditis elegans* propiciará a possibilidade de determinar o grau de toxicidade e seus mecanismos de ação em um organismo vivo, com resultados mais rápidos, reduzindo a utilização de mamíferos.

3. OBJETIVOS

Objetivo geral

Avaliar os efeitos tóxicos da exposição aguda à Fe_3O_4@Ag-NPs sintetizadas de forma biogênica no modelo alternativo *Caenorhabditis elegans*.

Objetivos específicos

- Verificar se a exposição aguda às Fe_3O_4-NPs, Ag-NPs e Fe_3O_4@Ag-NPs altera de maneira significativa parâmetros inicias de toxicidade;
- Observar se a exposição aguda às Fe_3O_4@Ag-NPs altera parâmetros reprodutivos dos nematoides;
- Analisar se há formação de corpos apoptóticos na linha germinativa após a exposição à Fe_3O_4@Ag-NPs em *C. elegans*;
- Determinar alterações locomotoras em *C. elegans* expostos à Fe_3O_4@Ag-NPs;
- Investigar o possível mecanismo envolvido na toxicidade gerada pela exposição Fe_3O_4@Ag-NPs através da avaliação do sistema colinérgico e dopaminérgico;
- Avaliar o sistema antioxidante de *C. elegans* expostos à Fe_3O_4@Ag-NPs.

4. CONCEITOS GERAIS E REVISÃO DE LITERATURA

4.1 Nanopartículas

Partículas em escala nanométrica têm sido utilizadas em grandes áreas como o setor energético, ambiental e na biomedicina (GHAZANFARI *et al.*, 2016; PIERETTI *et al.*, 2019). Sua importância se dá pela diferença de comportamento de outras partículas de mesma composição, principalmente devido às suas propriedades físico-químicas únicas, aos efeitos de tamanho, às propriedades magnéticas e eletrônicas, o papel desempenhado nas superfícies e suas excelentes propriedades ópticas (WU *et al.*, 2019). Nanopartículas (NPs) são comumente classificadas como partículas que variam de 1-100 nm, no entanto, existem muitos nanomateriais relatados que atingem 500 nm, dependendo da sua composição, aplicação e as diferentes propriedades apresentadas

em relação à sua estrutura (ARRUEBO *et al.*, 2007; NANOPARTICLES PROMISES AND RISKS, 2015). As NPs podem ser obtidas a partir de materiais inorgânicos ou materiais orgânicos (por exemplo, poliméricos ou lipídicos), que podem ou não ser biodegradáveis (ARRUEBO *et al.*, 2007).

Os avanços obtidos em pesquisas sobre síntese e caracterização de NPs facilitam a utilização em grande escala de produtos baseados em nanotecnologia, o que levou ao aumento do interesse de estudos nessa área (SAIFI; KHURANA; GODUGU, 2018). Aplicações biomédicas requerem NPs metálicas constituídas por "núcleo-casca", que consistem em um metal ou núcleo de óxido metálico, encapsulado em um revestimento inorgânico ou polimérico que torna as partículas biocompatíveis, estáveis e que podem servir como suporte para biomoléculas (ARRUEBO *et al.*, 2007). Suas propriedades magnéticas permitem que essas partículas possam ser usadas em inúmeras aplicações como agentes de contraste magnético na ressonância magnética (RM); agentes de hipertermia e vetores magnéticos que podem ser direcionados por meio de um gradiente de campo em direção a um determinado local, como no caso do direcionamento de medicamentos; além de favorecer a atividade antimicrobiana, oportunizando a solução de problemas de resistência de alguns microorganismos a antibióticos (JURGONS *et al.*, 2006; RODRIGUES *et al.*, 2019; SAIFI; KHURANA; GODUGU, 2018). Além disso, as NPs metálicas possuem facilidade para se anexar em células e tecidos para funcionalização, o que possibilita maiores ações biológicas (SALVATI; STELLACCI; KROL, 2015).

Entretanto, seus efeitos também podem trazer consequências negativas quando se acumulam nos tecidos (BOEY; HO, 2020). O fígado é um dos orgãos mais afetados pela exposição a NPs, seguido do baço e rins (POON *et al.*, 2019), embora estudos mostrem que NPs metálicas também proporcionaram benefícios terapêuticos surpreendentes para a saúde destes órgãos (BOEY; HO, 2020). As Ag-NPs, por exemplo, apresentaram efeitos protetores para hepatotoxicidade induzida por acetaminofeno em ratos através da redução da peroxidação lipídica hepática e restauração dos níveis de enzimas hepáticas, promovendo a regeneração dos hepatócitos (RESHI *et al.*, 2017). Considerando as aplicações da nanotecnologia, esta também surge como uma ferramenta relevante para fornecer opções terapêuticas ao

cérebro, visto que doenças como Parkinson, Alzheimer e Huntington têm incidência global e poucas opções terapêuticas (WONG; WU; BENDAYAN, 2012). Um dos obstáculos para ação de NPs no cérebro é a barreira sangue-cérebro (WOHLFART; GELPERINA; KREUTER, 2012). Para facilitar a penetração nos tecidos, a superfície das NPs pode ser projetada com anticorpos e peptídeos, podendo atingir diretamente as mitocôndrias dos neurônios e amenizar o estresse oxidativo que induziria a morte neuronal (KWON *et al.*, 2016).

4.1.1 Nanopartículas metálicas de Fe_3O_4 e Ag

As NPs de Fe_3O_4, também conhecidas como NPs de magnetita, possuem propriedades magnéticas únicas que possibilitam sua aplicação nas mais diversas áreas, recebendo atualmente um enfoque considerável. Destacam-se aplicações biomédicas como em diagnósticos, ressonância magnética por imagem, terapia antitumoral, transporte controlado de fármacos, separação de células e detecção de acido desoxirribonucleico (ADN) (GHAZANFARI *et al.*, 2016; HUSSEIN MONTAZERAN; SABER-SAMANDARI; KHANDAN, 2018; YANG *et al.*, 2004). Estudos mostram que estas nanopartículas apresentam baixa toxicidade e facilidade de funcionalização da superfície, o que possibilita o direcionamento de fármacos. As Fe_3O_4-NPs podem ser guiadas, através da aplicação de um campo magnético externo, até o alvo de interesse, por exemplo, um tecido tumoral e regiões infeccionadas por bactérias, fungos ou parasitas (HADDAD *et al.*, 2016; RODRIGUES *et al.*, 2019). Um dos seus potenciais mecanismos seria a produção de espécies reativas de oxigênio (ERO) induzidas por essas nanopartículas através da formação de radical hidroxila, uma ERO altamente reativa, em sistemas biológicos via reações de Fenton (1) e Haber-Weiss (2) (Figura 1).

$$Fe^{3+} + O_2^{\cdot -} \rightarrow Fe^{2+} + O_2$$

$$Fe^{2+} + H_2O_2 \rightarrow Fe^{3+} + OH^- + OH^{\cdot} \quad (1)$$

$$O_2^{\cdot -} + H_2O_2 \rightarrow O_2 + OH^- + OH^{\cdot} \quad (2)$$

Figura 1. Reações de Fenton (1) e Haber-Weiss (2) (MAI; HILT, 2019).

As Ag-NPs são amplamente estudadas atualmente. São as nanopartículas mais utilizadas do ponto de vista industrial e comercial e atraem um grande interesse científico devido as suas propriedades características: estabilidade química, maleabilidade, flexibilidade, elevadas condutividades elétrica e térmica, atividade catalítica, relativo baixo custo de produção e principalmente potente ação antimicrobiana frente a bactérias, vírus, fungos e protozoários (DURÁN *et al.*, 2018). Sua atividade antimicrobiana inicia pela interação físico-química das Ag-NPs com a superfície celular, o que leva à desestabilização e perfuração da membrana microbiana, além de danos causados pela geração de ERO ou pela inativação de macromoléculas como enzimas e proteínas a partir da liberação de íons Ag^{+} (DURÁN *et al.*, 2018; TUNG *et al.*, 2016).

Com o objetivo de combinar as propriedades das Fe_3O_4-NPs com as características já amplamente conhecidas das Ag-NPs, realizou-se a síntese biogênica de Fe_3O_4@Ag-NPs (PIERETTI *et al.*, 2019), visando uma estratégia para obtenção de um nanomaterial com propriedades específicas combinadas (BAEZA; GUILLENA; RAMÓN, 2016; TUNG *et al.*, 2016).

4.1.2 Nanopartículas híbridas de Fe_3O_4@Ag

A obtenção de nanomateriais híbridos vem apresentando um promissor avanço em relação às nanopartículas monofuncionais, o que possibilita a combinação de diferentes características e funções em uma única nanoestrutura, melhorando seu potencial de aplicação de nanomateriais na tecnologia, biomedicina e meio ambiente (SANVICENS; MARCO, 2008).

Uma estrutura híbrida de Fe_3O_4-NPs e Ag-NPs possibilita a obtenção de superparamagnetismos em função da presença de Fe_3O_4-NPs e potente ação antimicrobiana e antitumoral em função da presença de Ag-NPs (TUNG *et al.*, 2016). Estudos indicam um aumento da atividade antibacteriana das Fe_3O_4@Ag-NPs quando comparada aos efeitos das nanopartículas isoladas, além de um aumento da penetração das nanopartículas na superfície bacteriana de *Staphylococcus aureus*

(concentração). Isso ocorre devido a forte liberação dos íons Ag^{+} e Fe^{2+}, indicando um potencial efeito para aplicações biomédicas (TUNG *et al.*, 2016). Dados da literatura mostram que o tratamento utilizando Fe_3O_4@Ag-NPs apresentou toxicidade frente a linhagem de células tumorais e não tumorais, indicando uma dose dependência na redução da viabilidade celular. Entretanto, a porcentagem de células viáveis foi maior em todas as concentrações na linhagem celular não tumoral, o que indica uma seletividade para células tumorais (PIERETTI *et al.*, 2019).

A síntese dessas nanopartículas pode ser feita a partir da redução biogênica das Ag-NPs na superfície das Fe_3O_4-NPs através do uso de bactérias, fungos, ou extratos de plantas ou algas. A utilização de extratos de plantas é uma estratégia com grande potencial redutor conferido por diversas moléculas presentes nas plantas, como polifenóis, o que tem como vantagem adicional diminuir o uso de solventes tóxicos, reduzindo impactos no meio ambiente. Essas moléculas impedem a agregação das nanopartículas e desempenham um importante papel na estabilização do nanossistema (SEABRA; DURÁN, 2015). O extrato de *Camellia sinensis* (chá verde) destaca-se por apresentar um potencial para a síntese de nanopartículas, pois é rico em catequina, metabólito secundário que consiste em um agente redox polifenólico encontrado em plantas (Figura 2) (ROLIM *et al.*, 2019). Entretanto, a segurança destas NPs é desconhecida, sendo necessárias maiores investigações que possibilitem o esclarecimento de seus mecanismos de ação *in vivo*.

Figura 2. Esquema de síntese de Fe_3O_4@Ag-NPs (PIERETTI *et al.*, 2019).

4.2 Nanotoxicologia

Com o aumento do uso de nanotecnologia em produtos comerciais, o estudo sobre a interação de nanomateriais com os sistemas biológicos se torna necessário, buscando desvendar os mecanismos de ação frente a proteínas e células a fim de auxiliar no desenvolvimento de áreas ambientais e biomédicas (SUH *et al.*, 2009). Esse estudo da toxicologia dedicado a pesquisa dos efeitos toxicológicos de nanomateriais em diferentes sistemas biológicos, incluindo células, tecidos e organismos vivos é denominado nanotoxicologia (SELVARAJ *et al.*, 2018).

De acordo com a literatura, a maioria dos tipos de NPs pode penetrar nos tecidos e células por diferentes rotas, incluindo inalação, injeção, ingestão e via cutânea, penetrando membranas celulares, o que pode resultar em danos severos(SAIFI; KHURANA; GODUGU, 2018; WU *et al.*, 2019). A exposição ocupacional a NPs em seres humanos em locais como laboratórios, indústrias, serviços telefônicos, emissão por veículos automotores, soldagem e pintura é uma das causas de contaminação por nanomateriais, gerando riscos à saúde destes trabalhadores (SAIFI; KHURANA; GODUGU, 2018). Em relação à exposição ambiental, NPs de metais e óxido de metais, por exemplo, podem entrar na água por vários meios, como por exemplo, descarga direta ou descarga de resíduos. Essas partículas possuem boa dispersibilidade e estabilidade sob a ação da matéria orgânica na água e podem adentrar em organismos aquáticos como peixes através da cadeia alimentar. Como consequência, o uso de produtos contaminados por humanos pode gerar o acúmulo destas substâncias no organismo (BAI; TANG, 2020). Devido a isso, é necessário encontrar métodos e modelos eficientes para avaliar a biossegurança de NPs.

Existem modelos experimentais alternativos promissores para a avaliação toxicológica de nanomateriais, como *Danio rerio* (peixe-zebra), *Drosophila melanogaster* (mosca da fruta) e *Caenorhabditis elegans*. Estudos toxicológicos de várias NPs usando o modelo de peixe-zebra e seus embriões são cada vez mais utilizados, uma vez que são modelos que detectam e respondem a poluentes e metais pesados no meio ambiente (YIN *et al.*, 2018). Os testes em embriões de peixes foram

reconhecidos como uma alternativa promissora ao teste clássico de toxicidade aguda devido a vantagens como transparência durante as fases embrionárias (BAI; TANG, 2020; EMBRY *et al.*, 2010). A *Drosophila melanogaster* permite uma avaliação rápida de NPs, devido ser um modelo experimental de fácil manutenção com um curto ciclo de vida. Estudos demonstraram toxicidade de Ag-NPs em *Drosophila melanogaster* levando a diminuição de sua sobrevivência e reprodução (POSGAI *et al.*, 2011).

Segundo Saifi et al. (2018), “nanotecnologia, nanomedicina, e nanotoxicologia são três faces do mesmo triângulo que visam a melhoria da vida humana”. Atualmente as normas para a avaliação toxicológica de NPs ainda não estão totalmente definidas (SAIFI; KHURANA; GODUGU, 2018), entretanto a Organização para a Cooperação e Desenvolvimento Econômico (OCDE) auxilia os países na implementação de políticas nacionais que garantam o desenvolvimento responsável de nanotecnologias (OECD, 2007). Além disso, a NanoReg, projeto de pesquisa para regulamentação em nanotecnologia proposto pela União Europeia, no qual o Brasil faz parte, também tem como objetivo disponibilizar aos legisladores um conjunto de ferramentas para o desenvolvimento de estratégias de avaliações de risco do uso de nanomateriais e estabelecer uma colaboração entre governos e indústrias para gestão adequada e criação de abordagens comuns para avaliação de nanosegurança (MIINISTÉRIO DA CIÊNCIA E TECNOLOGIA, 2021). Essas políticas focam na segurança e avaliação de nanomateriais para garantir a saúde humana e segurança ambiental, envolvendo testes para avaliação de riscos (RASMUSSEN *et al.*, 2016). A carência de dados sobre a segurança de produtos provenientes de partículas nanométricas faz necessária maiores investigações *in vivo*.

4.3 *Caenorhabditis elegans*

Buscando elucidar mecanismos relacionados à biologia molecular e diminuir o uso de vertebrados na pesquisa, o nematóide *Caenorhabditis elegans* vem sendo amplamente estudado desde 1963. Devido a simplicidade genética do verme, o biólogo Sydney Brenner propôs que o nematóide *C. elegans* seria um ótimo modelo para resolver as limitações de outros modelos experimentais (CORSI, Ann K.;

WIGHTMAN; CHALFIE, 2015).

O *C. elegans* é um pequeno nematoide, não parasita, de vida livre. Quando adulto mede aproximadamente 1 mm de comprimento, pertence à família Rhabditidae, que se alimenta de bactérias presentes em matéria orgânica em decomposição. No ambiente laboratorial é mantido em placas de petri com meio de crescimento para nematoide (NGM- nematode growth medium) e *Escherichia coli* como fonte de alimento, a 20 ºC. Este modelo alternativo apresenta 38% dos genes de codificação de proteínas ortólogos ao genoma humano, 60-80% dos genes humanos tem um ortólogo no genoma de *C. elegans* e 40% dos genes associados a enfermidades humanas estão claramente presentes no verme (CORSI, Ann K; WIGHTMAN; CHALFIE, 2015; TEJEDA-BENITEZ; OLIVERO-VERBEL, 2016). Uma das grandes vantagens do modelo é a sua reprodução, este nematoide é encontrado nas formas hermafrodita e macho, sendo sua forma hermafrodita 99.9% da população, a qual faz a postura de 200 a 300 ovos a cada ciclo de vida. O verme passa por 4 estágios larvais até se tornar adulto, isso dura aproximadamente 4 dias em temperatura ambiente, com uma longevidade de 12 a 20 dias (GILES; RANKIN, 2009) (Figura 3). Quando há uma diminuição da oferta de alimento no ambiente em que o verme se encontra, a forma L1 não segue o seu ciclo normal, entrando em um estágio intermediário, chamado larva dauer. Essa forma pode viver meses sem comida e irá continuar seu ciclo normalmente após encontrar condições adequadas de alimentação (TEJEDA-BENITEZ; OLIVERO-VERBEL, 2016).

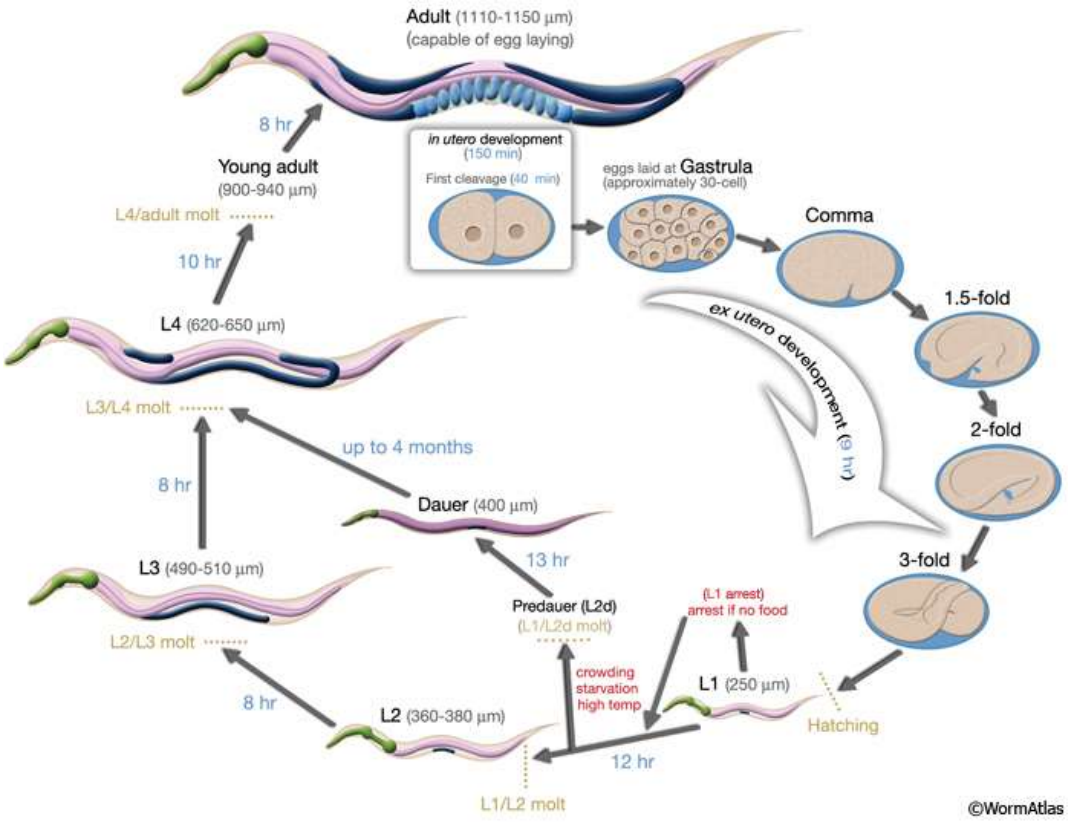

Figura 3. Ciclo de vida do nematóide *Caenorhabditis elegans* (Fonte: WormAtlas).

Por ter o seu genoma completamente sequenciado, há uma maior facilidade para realização de manipulações genéticas para geração de animais nocaute e transgênicos, expressando proteína verde fluorescente (“*green fluorescence protein”* GFP) dessa forma, marcando proteínas de interesse. Associado ao corpo transparente é possível visualizar *in vivo* neurônios, expressão de enzimas e tráfego de fatores de transcrição tornando o modelo promissor para avaliação de segurança (Figura 4) (GONZALEZ-MORAGAS; ROIG; LAROMAINE, 2015).

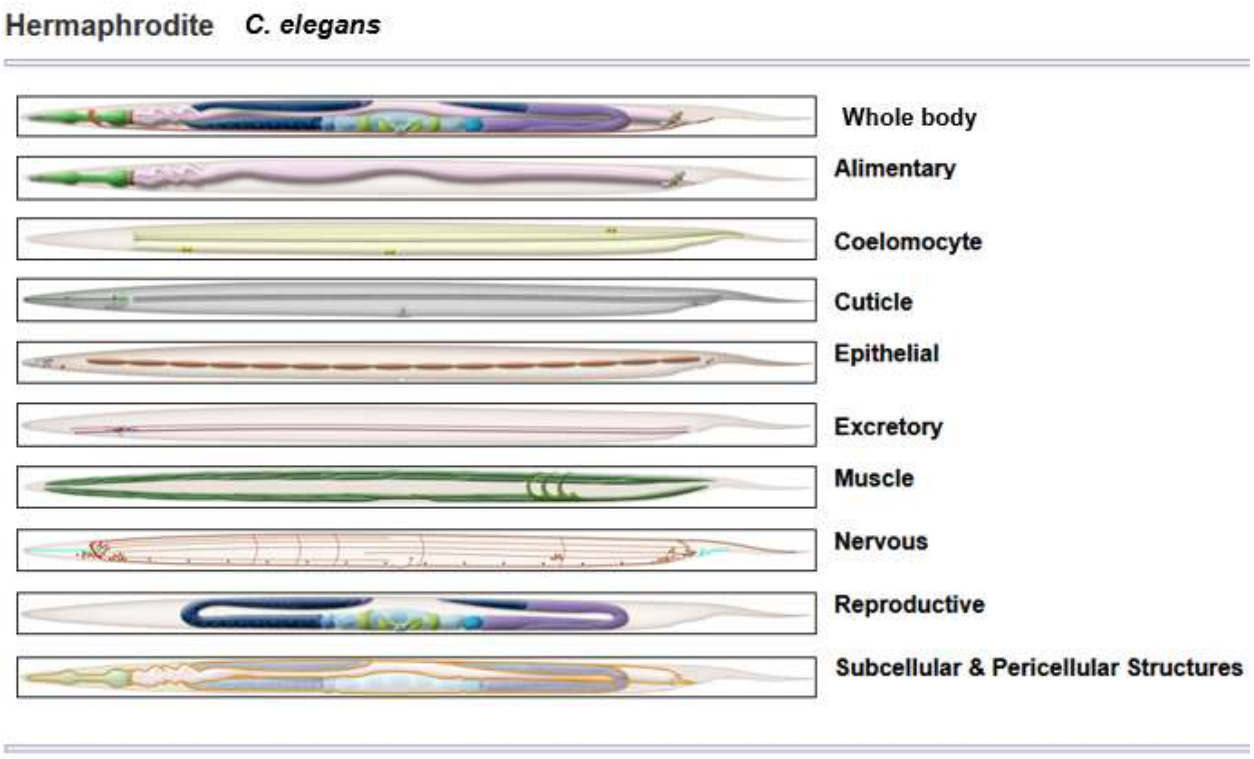

Figura 4. Estrutura corporal de *Caenorhabditis elegans* hermafrodita (Imagem adaptada de WormAtlas).

A reprodução, bem como a postura de ovos de *C. elegans* são "*endpoints*" toxicológicos estudados há décadas e estudos mostram que agentes tóxicos podem reduzir (RINGSTAD; HORVITZ, 2008; TESHIBA; MIYAHARA; TAKEYA, 2016) ou aumentar esses parâmetros (EMERSON *et al.*, 2021; HARDAKER *et al.*, 2001). O comportamento de postura de ovos de *C. elegans* é controlado por um pequeno circuito de neurônios que consiste em dois neurônios serotoninérgicos (HSNs) e seis neurônios colinérgicos ventrais C (VCs) (Figura 5), que fazem sinapses em um conjunto de músculos vulvares cuja contração expele os ovos (COLLINS *et al.*, 2016; FAGAN; PORTMAN, 2014; SCHAFER, 2006). Sabe-se que os músculos vulvares são excitados ritmicamente de maneira conjunta com as curvas do corpo dos nematoides. Isso se da pela sinalização dos neurônios motores colinérgicos, incluindo os VCs, que são ativados durante a locomoção (COLLINS *et al.*, 2016; WEINSHENKER; GARRIGA; THOMAS, 1995).

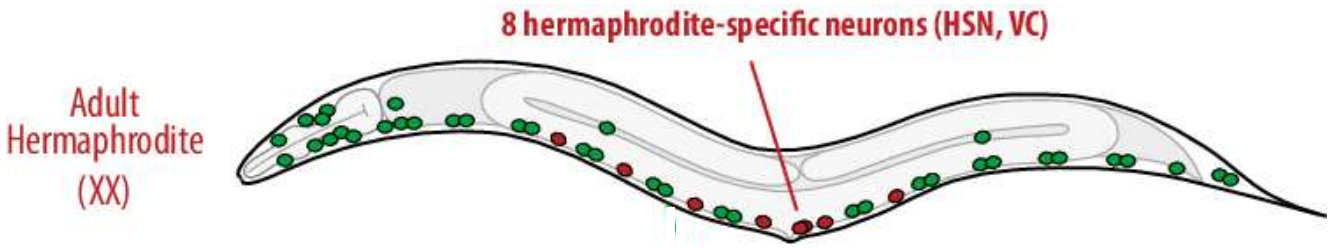

Figura 5. Neurônios serotoninérgicos (HSN) e neurônios colinérgicos ventrais C (VC) de *C. elegans* hermafrodita (Imagem adaptada de FAGAN; PORTMAN, 2014).

A via de sinalização tipo insulina / IGF-1 (“insulin-like growth factor”) de *C. elegans* é regulada por ligantes semelhantes à insulina que se ligam ao ortólogo de mamíferos DAF-2 do receptor transmembrana da insulina (IGFR) / IGF-1. A ativação de DAF-2 / IGFR resulta na ativação da fosfoinositídeo 3-quinase AGE-1 / PI3K e, com isso, proteínas quinases serina / treonina PDK-1, AKT-1 e AKT-2 são ativadas. No entanto, quando a via de sinalização de insulina está inativada (na ausência de ligantes tipo insulina), ocorre a migração do fator de transcrição DAF-16 (homólogo a FoxO em mamíferos) do citoplasma para o núcleo celular, onde exerce seus efeitos (Figura 6) (MURPHY; HU, 2013; ROHN *et al.*, 2018; SUN; CHEN; WANG, 2017). Além disso, DAF-16 / FoxO interage com fatores nucleares adicionais, incluindo HSF-1 (ortólogo do HSF1 humano - fator de transcrição de choque térmico 1) e SKN-1 (ortólogo a Nrf1/2/3 em mamíferos), levando à expressão de enzimas detoxificantes como Mn-SODs (superóxido dismutase), catalase (CAT), GSTs (glutationa-S-transferase) e GPX (glutationa peroxidase) (MURPHY; HU, 2013).

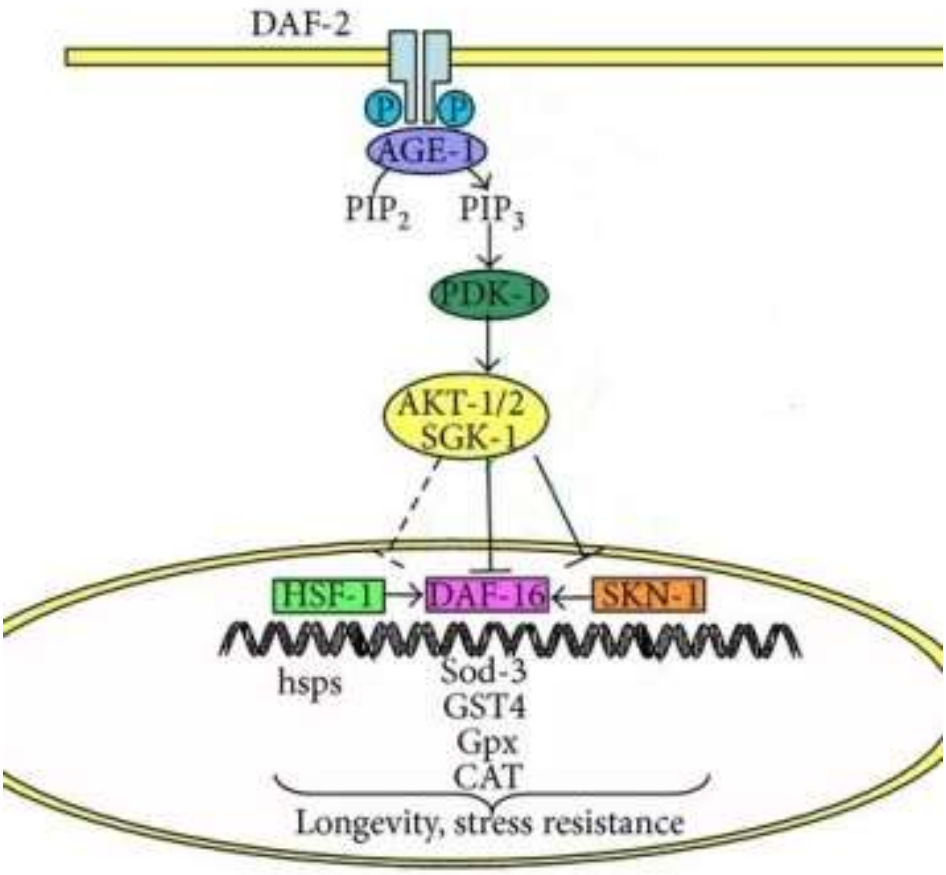

Figura 6. Via de sinalização da insulina em *C. elegans* (Imagem adaptada de KOCH *et al.*, 2014).

Dentre as vias de sinalização estudadas em *C. elegans* está a apoptose celular, visto que a remoção de células apoptóticas é essencial para a evolução fisiológica e funcionamento normal do organismo. Em *C. elegans*, o mecanismo de apoptose celular ainda não é bem compreendido, porém, sabe-se que o processo de apoptose inicia com a ativação de células EGL-1 que foram destinadas a morrer. EGL-1 é análoga de BH3 em mamíferos, que, quando ativada, inibe CED-9 (análogo de BCL-2 em mamíferos). CED-4 é análogo APAF-1 em mamíferos e serve como um ativador de CED-3, uma caspase, independente de EGL-1, que então leva a subsequente ativação de CED-1, CED-6 e CED-7, causando a morte celular (ARVANITIS *et al.*, 2013; GARTNER; BOAG; BLACKWELL, 2008). O receptor CED-1 reconhece um ligante desconhecido na célula apoptótica e sinaliza através de sua

cauda citoplasmática para a proteína adaptadora CED-6. CED-1, CED-6 e CED-7 são necessárias para a reorganização da actina em torno da célula apoptótica, a fim de causar o engolfamento da célula morta (Figura 7) (KINCHEN *et al.*, 2005).

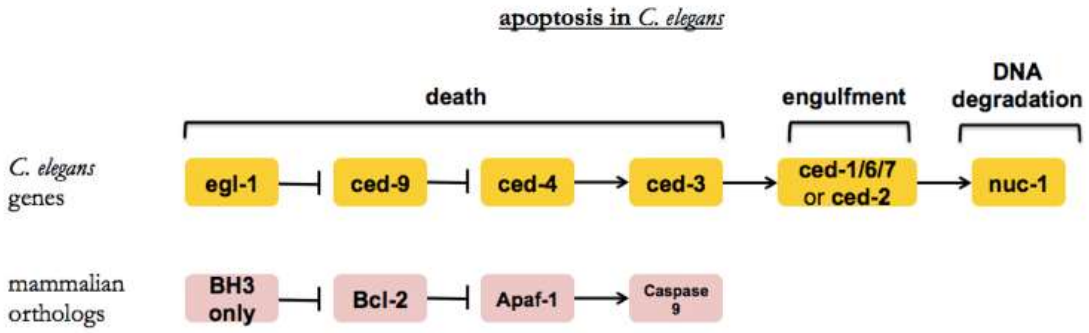

Figura 7. Via de sinalização de apoptose em *C. elegans* e em mamíferos (Fonte: CureFFI.org).

Com a crescente aplicação de NPs e o aumento da exposição a produtos provenientes da nanotecnologia estudos de avaliação de biossegurança de NPs utilizando *C. elegans* estão aumentando. *C. elegans* tornou-se um modelo alternativo promissor para avaliação toxicológica de nanomateriais, oferecendo uma opção para os pesquisadores investigarem os efeitos biológicos das NPs com menor custo e tempo, diminuindo a limitação de ensaios *in vitro* e os problemas éticos com o uso de mamíferos (WU *et al.*, 2019). Além disso, como é um modelo experimental bem conhecido, com alta sensibilidade a diferentes contaminantes, representa um importante bioindicador para níveis de contaminação de solo e ecossistemas aquáticos, sendo considerado um modelo com alto potencial para ser utilizado na avaliação de risco ambiental (QUEIRÓS *et al.*, 2019).

Os estudos avaliando as NPs de Fe e Ag isoladas demonstraram uma significativa toxicidade em *C. elegans*. Um estudo anterior avaliou NPs magnéticas de Fe_3O_4 (MNPs) obtidas por uma síntese verde com glutationa nos nematoides e observou que número de ovos postos por verme diminuiu, conforme o aumento da concentração de NPs. Este resultado pode ser consequência de inibição do seu desenvolvimento, fazendo com que os vermes não atinjam o estágio de adulto, no qual se tornam férteis (MARIMON-BOLÍVAR *et al.*, 2019). *C. elegans* expostos a Ag-

NPs apresentaram mudanças epigenéticas que são herdadas pela progênie não exposta (WAMUCHO; HEFFLEY; TSYUSKO, 2020). A inibição da reprodução segue uma relação dose-dependente, refletindo a modificação na transcrição de genes relacionados ao comportamento reprodutivo (KIM; NAM; AN, 2012; LUO *et al.*, 2016).

Estudos toxicológicos que avaliam NPs metálicas *in vitro* e *in vivo* ainda são escassos, e as normas para a avaliação toxicológica dessas NPs não estão totalmente definidas (SAIFI; KHURANA; GODUGU, 2018; WU *et al.*, 2019; ZIELIŃSKA *et al.*, 2020). Além disso, não existem estudos *in vivo* que demonstrem os efeitos de NPs híbridas em organismos vivos tornando necessário maiores investigações.

5. MATERIAIS, MÉTODOS E RESULTADOS

A metodologia, resultados e discussão dos resultados desta dissertação estão na forma de artigo, o qual foi publicado na revista Food and Chemical Toxicology.

Artigo

Food and Chemical Toxicology 179 (2023) 113945

Contents lists available at ScienceDirect

Food and Chemical Toxicology

journal homepage: www.elsevier.com/locate/foodchemtox

Iron oxide/silver hybrid nanoparticles impair the cholinergic system and cause reprotoxicity in *Caenorhabditis elegans*

Aline Castro Silva [a], Alisson Gleysson Rodrigues dos Santos [a], Joana Claudio Pieretti [b], Wallace Rosado Rolim [b], Amedea Barozzi Seabra [b], Daiana Silva Ávila [a,*]

[a] Graduate Program in Biochemistry, Laboratory of Biochemistry and Toxicology in Caenorhabditis Elegans, Federal University of Pampa, Uruguaiana, RS, Zip code 97500-970, Brazil

[b] Center for Natural and Human Sciences (CCNH), Federal University of ABC (UFABC), Santo André, SP, Zip code 09210-580, Brazil

ARTICLE INFO

Handling Editor: Dr. Bryan Delaney

Keywords:
Nanotoxicology
Metal NPs
Hybrid nanoparticles
Reproduction

ABSTRACT

Iron oxide nanoparticles present superparamagnetic properties that enable their application in various areas, including drug delivery at specific locations in the organism. Silver nanoparticles have potent antimicrobial effects. Although the combination of Fe_3O_4-NPs and Ag-NPs in one hybrid nanostructure (Fe_3O_4@Ag-NPs) demonstrated promising targeted biomedical applications, their toxicological effects are unknown and need to be assessed. *Caenorhabditis elegans* is a promising model for nanotoxicological analysis, as it allows an initial screening of new substances. After exposure to Fe_3O_4-NPs, Ag-NPs and Fe_3O_4@Ag-NPs, we observed that hybrid NPs reduced the *C. elegans* survival and reproduction. Higher concentrations of Fe_3O_4@Ag-NPs caused an increase in cell apoptosis in the germline and a decrease in egg laying, which was associated with a decrease in worm swimming movements and abnormalities in the cholinergic neurons. Fe_3O_4@Ag-NPs caused an increase in reactive oxygen species, along with activation of DAF-16 transcription factor. A higher expression of the target genes GST-4::GFP and SOD-3::GFP were evidenced, which suggests the activation of the antioxidant system. Our results indicate the reprotoxicity caused by high levels of Fe_3O_4@Ag-NPs, as well as cholinergic neurotoxicity and activation of the antioxidant system in *C. elegans*, suggesting that high concentrations of these nanomaterials can be harmful to living organisms.

1. Introduction

Nanotechnology has become a growing field of research, since the products obtained by this means have advantages over other products of the same molecular composition (Arruebo et al. 2007). These advantages of nanomaterials are mainly due to their properties related to the small size and the larger contact surface area, which confers unique properties when compared to bulk materials, with promising potential for application in various industrial fields. Metallic NPs consist of a metal or metal oxide core, with an inorganic or polymeric coating. Depending on their chemical composition, the NPs can have magnetic properties that make them of great interest in the biomedical field (Boey and Ho, 2020). Individually, Fe_3O_4 and Ag NPs have several documented biomedical applications (Burdusel et al. 2018; Montiel Schneider et al. 2022). Fe_3O_4-NPs have unique magnetic properties that enable their application in the most diverse areas such as imaging diagnostics, antitumor therapy and controlled drug transport (Ghazanfari et al., 2016; Hussein Montazeran et al., 2018; Montiel Schneider et al. 2022). Ag-NPs are currently widely studied, mainly due to their potent antimicrobial action (Burdusel et al. 2018; Durán et al. 2018). Studies indicate that hybrid nanomaterials (more than one metal) can present promising advances in relation to monofunctional NPs, as they combine the characteristics and functions of two metals in a single structure, providing progress for applications of nanomaterials with specific properties (Pieretti et al. 2019, 2019b, Pieretti et al., 2021a,b). In this sense, with the aim of combining the properties of Fe_3O_4-NPs with the already widely known characteristics of Ag-NPs, we have synthesized hybrid Fe_3O_4@Ag-NPs and demonstrated their superior cytotoxicity effect against cancer cells, compared to individually Fe_3O_4-NPs or Ag-NPs (Pieretti et al., 2019). In a subsequent study, we have demonstrated the successfully coating of Fe_3O_4@Ag-NPs with chitosan containing nitric oxide donor and their antibacterial, anticancer and hemocompatibility effects (Pieretti et al., 2021a,b).

* Corresponding author. Universidade Federal do Pampa, UNIPAMPA Programa de Pós-Graduação em Bioquímica, BR 472 – Km 592, Postal Code 118, Zip code 97500-970, Uruguaiana, RS, Brazil.
E-mail address: daianaavila@unipampa.edu.br (D.S. Ávila).

https://doi.org/10.1016/j.fct.2023.113945
Received 1 April 2023; Received in revised form 27 June 2023; Accepted 11 July 2023
Available online 13 July 2023

List of abbreviations

MNPs	Magnetic nanoparticles
NPs	Nanoparticles
PDI	Polydispersity index
nm	Nanometers
NGM	Nematode growth medium
SS	Stock suspension
ROS	Reactive oxygen species
carboxy-DCFH-DA	5(6)-carboxy-2′,7′-dichlorofluoroscein diacetate
GST-4	Glutathione-S-transferase 4
SOD-3	Superoxide dismutase 3
GSH	Reduced glutathione
CDNB	Dinitrochlorobenzene
Std	Standard
UHR	Ultra-high resolution
DNA	Deoxyribonucleic acid
VCs	ventral C neurons
IIS	Insulin-like growth factor signaling
IGFR	Transmembrane insulin-like receptor
PI3K	Phosphoinositide 3-kinase

However, the same properties that make nanomaterials attractive may also be responsible for harmful effects on living organisms when they distribute and accumulate in tissues (Dhawan and Sharma, 2010; Boey and Ho, 2020). Most types of NPs can penetrate tissues and cells by different routes, including inhalation, injection, ingestion, and skin (Saifi et al., 2018; Wu et al., 2019). In addition, factors such as pH, coating, synthesis route, or presence of humic substances play a significant role in their toxicokinetic, favoring or not penetration into cell membranes (Dhawan and Sharma, 2010).

As we have demonstrated that hybrid Fe_3O_4@Ag-NPs have higher toxicity against cancer cells and antibacterial effects, compared to individual Fe_3O_4-NPs or Ag-NPs, in this present study we deeply characterized their toxicity towards *Caenorhabditis elegans*, a promising model for nanotoxicological analysis. *Caenorhabditis elegans* has become a great tool for nanotoxicological studies, making it possible to evaluate the impacts of these products on a variety of systems, including the nervous, digestive, immune, and reproductive. It is transparent, of easy handling and maintenance, in addition to having excellent molecular and genetic characteristics, which allows the results to contribute to advances in the environmental and biomedical areas (Tejeda-Benitez and Olivero-Verbel, 2016; Singh et al. 2023). Previous studies using *C. elegans* reported a concentration-dependent increase in mitochondrial superoxide dismutase (SOD-3) expression after exposure to Ag-NPs, which was associated with a significant reduction in fertility (Roh et al. 2009). Inhibition of reproduction caused by Ag-NPs also followed a dose-dependent relationship, reflecting the modification in the transcription of genes related to reproductive behavior (Roh et al. 2009; Kim et al. 2012; Luo et al. 2016). However, Spagnoletti et al., 2021 reported the safety of biogenically synthesized Ag-NPs in the development and reproduction of *C. elegans* in relation to chemically synthesized (Spagnoletti et al. 2021). Fe_3O_4-NPs obtained by green synthesis increased *C. elegans* mortality, reducing nematodes size and locomotion (Patiño-Ruiz et al. 2020). In the case of hybrid synthesis, few data are found in the literature, and most of the studies address the synthesis and characterization and not their biological activity. Many gaps still need to be clarified for a better understanding of the effects of Fe_3O_4@Ag-NPS *in vivo*.

In this study, we investigated the effects of biogenically synthesized Fe_3O_4@Ag-NPs using the *in vivo C. elegans* model. We elucidated the action of hybrid NPs in the reproductive, neuronal and also the antioxidant system by evaluating the levels of reactive oxygen species together with the modulation of the DAF-16 redox-related pathway.

2. Material and methods

2.1. Chemicals

For the synthesis of nanoparticles, we use iron chloride II tetrahydrate ($FeCl_2{\bullet}4H_2O$), iron chloride III hexahydrate ($FeCl_3{\bullet}6H_2O$), and silver nitrate ($AgNO_3$) were obtained from Sigma-Aldrich (St. Louis, MO, USA). Hydrochloric acid (HCl), ethanol, ammonium hydroxide (NH_4OH), and sodium hydroxide (NaOH) were acquired from Labsynth (Diadema, SP, Brazil). The green tea powder (*Camellia Sinensis*) was purchased from Sumioka Shokuhin Kabushikikaisha Hiraguti (Japan). Nanoparticles were synthesized using analytical grade water, purified by reverse osmosis purifier DV25 from ELGA (Ontario, Canada). For the *C. elegans* analyzes we use levamisole (RIPERCOL® L 150F; SP, Brazil); 5(6)-carboxy-2′,7′-dichlorofluoroscein diacetate (carboxy-DCFH-DA, Sigma Aldrich; CAS: 127770-45-0; RS, Brazil); reduced glutathione (GSH, Sigma Aldrich; CAS: 70-18-8; Brazil, RS); 1-chloro-2,4-dinitrobenzene (CDNB, Sigma Aldrich; CAS: 97-00-7; RS, Brazil); coomassie brilliant blue G-250 (Sigma Aldrich; CAS: 6104-58-1; RS, Brazil). All other reagents were of analytical grade and were obtained from local suppliers.

2.2. Nanoparticles synthesis

Fe_3O_4-NPs were synthesized by chemical co-precipitation of Fe^{2+}/Fe^{3+} method, and fully characterized Ag-NPs were synthesized by green tea extract, while Fe_3O_4@Ag-NPs were obtained by similar protocol, through the reduction of silver ions on the surface of Fe_3O_4-NPs using green tea extract, as previously reported (Pierretti et al. 2019). A Zetasizer nanoseries (Malvern Instruments, UK) coupled with a 633 nm laser and adjusted with a backscattered angle of 173° was employed for analyzing hydrodynamic parameters. All measurements were performed in triplicate, in plastic cuvettes and disposable folded capillary zeta cell (10 mm path length). The morphology and size distribution of Fe_3O_4-NPs, Ag-NPs and Fe_3O_4@Ag-NPs in solid state was obtained by a transmission electron microscope (JEM-2100-JEOL LaB6) operating at ultra-high resolution (UHR). The powdered sample was prepared using a grid and analyzed at an angle of 42°. The micrographs were analyzed using Image J (NIH, Bethesda, MD, USA) software for Windows, generating a size histogram.

2.3. C. elegans strains and maintenance

Worms were cultivated in Petri dishes containing nematode growth medium (NGM) (Stiernagle, 2006) and fed with *Escherichia coli* OP50 under controlled temperature (20 °C) and humidity (>95%) (Panasonic Healthcare company of North America, MIR-254-PA). The population was synchronized to obtain all worms at the same larval stage. For this, we used a bleaching solution (NaOH 1M, NaClO 1%, and distilled H_2O) to break the cuticle of pregnant hermaphrodites and release the eggs. All the strains employed were submitted to the same process. The strains used consisted of N2 (wild type), MD701 bcIs39 [*lim-7*p::*ced-1*::GFP + *lin-15*(+)] V, LX929 vsIs48 [*unc-17*::GFP], BY200 vtIs1 [*dat-1*p::GFP; *rol-6*(su1006)], CL2166 dvIs19 [(pAF15)*gst-4*p::GFP::NLS] III, CF1553 muIs84 [(pAD76)*sod-3*p::GFP + *rol-6*(su1006)] and TJ356 zIs356 [*daf-16*p::*daf-16*a/b::GFP + *rol-6*(su1006)] IV. The strains of *C. elegans* and *E. coli* were obtained from the *Caenorhabditis* Genetics Center (CGC, Minnesota, USA). BY200 strain was donated by Dr. Michael Aschner (Director, Einstein Center of Toxicology).

2.4. Exposure protocol

For the treatment, 0.010 g of NPs (Fe_3O_4-NPs, Ag-NPs, or Fe_3O_4@Ag-

NPs) were dispersed in 1 mL of distilled water, obtaining a stock suspension (SS) of 10,000 μg mL^{-1}. This SS was placed in the ultrasound bath at room temperature for 1 h. From this SS, two dispersions were prepared, for which 20 μL and 40 μL were pipetted, respectively, in microtubes, topped up with distilled water to 2 mL. From these dispersions, final concentrations of 1, 10, 50 and 100 μg mL^{-1} of NPs were obtained, to which the worms were exposed (Fig. 2S).

We used 1500 or 3000 worms treated at the first (L1; −14 h after synchronization) or fourth (L4; −48 h after L1) larval stage. The number of worms and the larval stage were chosen according to the need for the analysis. For all experiments, the animals were acutely exposed to NPs (Fe_3O_4-NPs, Ag-NPs, or Fe_3O_4@Ag-NPs) for 30 min, in distilled water. For the analysis of survival rate, body length and brood size, the effect of these three NPs (Fe_3O_4-NPs, Ag-NPs and Fe_3O_4@Ag-NPs) were evaluated using the following groups: control (exposed only to distilled water) and treated with NPs at 1, 10, 50 and 100 μg mL^{-1}. Due to the lack of information on hybrid NPs in the literature, we chose concentrations based on previous studies using individualized Fe_3O_4 and Ag NPs (Roh et al. 2009; Lim et al. 2012; Yang et al. 2016; Pierretti et al. 2019; Amigoni et al. 2021). The other tests were performed only with the hybrid NPs (Fe_3O_4@Ag NPs) at concentrations 1, 10 and 50 μg mL^{-1}, once significant toxicity was observed at 100 μg mL^{-1}. After exposure, the worms were washed with saline (NaCl 0.5%) in three steps, then placed on NGM plates seeded with *E. coli* OP50 as a food source.

2.5. Survival rate

To verify whether the NPs demonstrate potential toxicity, we evaluated the strain N2 48 h after the treatment with Fe_3O_4-NPs, Ag-NPs or Fe_3O_4@Ag-NPs and scored the live worms. Three experiments were performed individually in duplicates using 1500 worms at L1 stage. The worm population was estimated by counting an area delimited by quadrants, using a stereomicroscope (Leica S8 Apo Stereomicroscope, SP, Brazil). The number of surviving animals were normalized by the total number of worms in the control group (percentage of control). Assays were repeated at least three times. LD_{50} (lethal dose 50%) values extrapolation for mammals was calculated from the experimental LC_{50} (lethal concentration 50%) obtained for Fe_3O_4@Ag-NPs during the lethality assays by using the regression function described at ICCVAM (2006):

$$Log(LD_{50}) = 0.439*log(LC_{50}) + 0.621$$

2.6. Body length assay

After 48 h of NPs exposure, the nematodes were collected with distilled water and transferred to microtubes, washed 3 times with distilled water after natural sedimentation. Then, the worms were transferred to glass slides containing levamisole (1 mM) and covered with coverslips to obtain images using a Nikon Eclipse 50i microscope (Nikon, Tokyo, Japan). Image J (NIH, Bethesda, MD, USA) software for Windows was used to measure nematode body length from head to tail. The body length was normalized by the body length of the control group worms (percentage of control). Each concentration group evaluated 5 nematodes and at least three independent experiments were performed.

2.7. Brood size assay

The reproductive capacity of *C. elegans* can be assessed by brood size (Qu et al. 2019). After 48 h of exposure to NPs, nematodes from each group (including control) were transferred to plates containing NGM and *E. coli* OP50 seeded in the center of the plate. The worms were individually transferred to new NGM plates every 24 h until the end of the reproductive period. Using a stereomicroscope (Leica S8 Apo Stereomicroscope, SP, Brazil), the size of the progeny of the worms was recorded daily. The brood size was normalized by the brood size of the control group worms (control percentage). The experiments were performed in triplicates and at least three independent experiments were

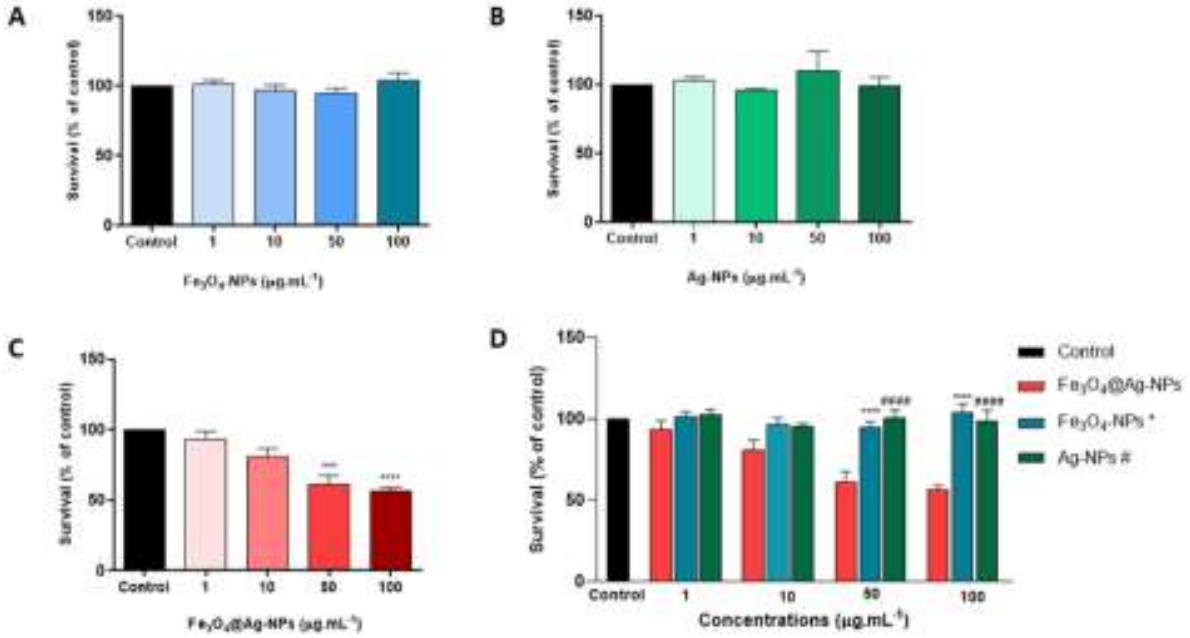

Fig. 1. Survival rate decreased after exposure to Fe_3O_4@Ag-NPs. Survival rate of worms exposed to different concentrations of (A) Fe_3O_4-NPs (n = 6); (B) Ag-NPs (n = 3); (C) Fe_3O_4@Ag-NPs (n = 4) after 48 h of the end of exposure (L4 stage). Data were expressed as mean ± standard error of mean (SEM). The analysis of the survival rate for Fe_3O_4-NPs was performed by nonparametric Kruskal-Wallis test. For survival analysis of worms exposed to Ag-NPs and Fe_3O_4@Ag-NPs was performed One-way ANOVA. Using Tukey's multiple comparison test for the Fe_3O_4@Ag-NPs analysis. (*) Indicates a statistically significant difference in relation to the control group with $^{***}p < 0.001$; $^{****}p < 0.0001$. In (D) is represented the survival rate between the three NPs (n = 3). (*) Indicates a statistically significant difference between Fe_3O_4@Ag-NPs and Fe_3O_4-NPs with $^{****}p < 0.0001$. (#) Denotes a statistically significant difference between Fe_3O_4@Ag-NPs and Ag-NPs with $^{####}p < 0.0001$ by One-way ANOVA followed by Tukey's multiple comparison test.

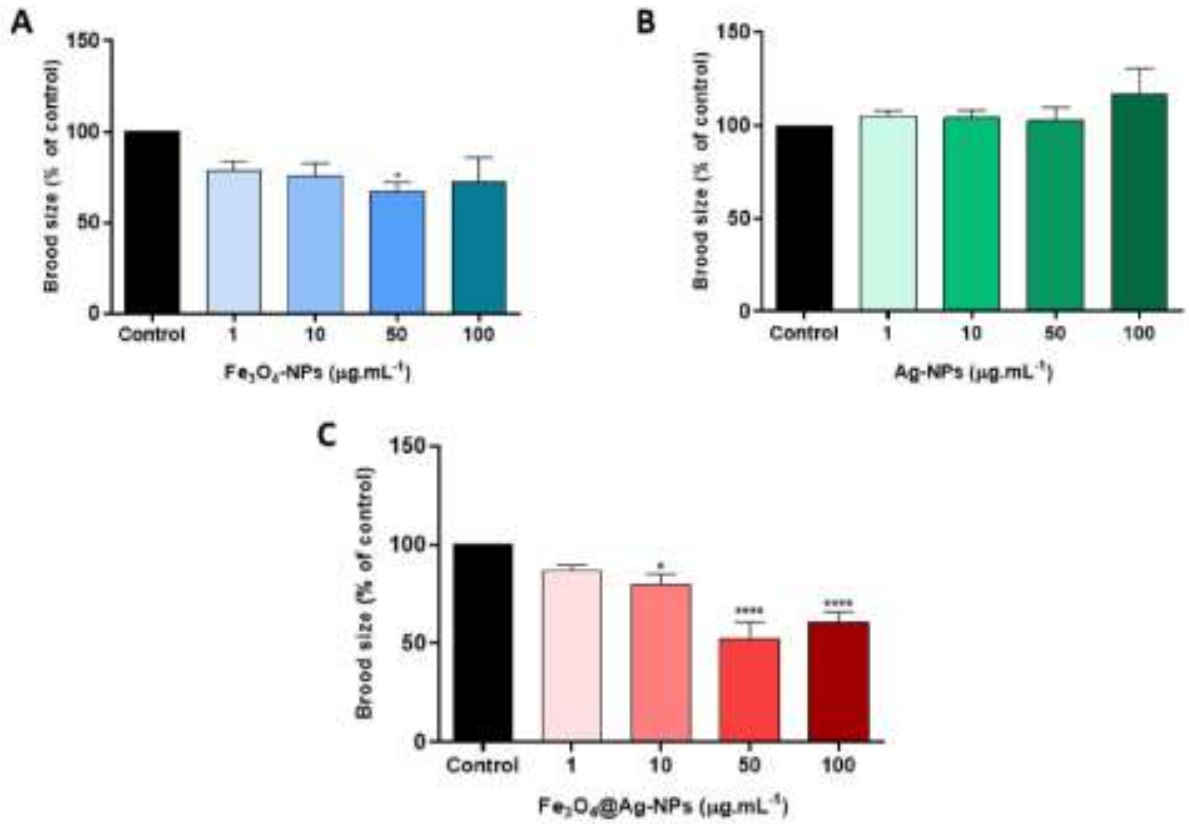

Fig. 2. Brood size decreased after exposure to Fe_3O_4@Ag-NPs. Total brood size of worms exposed to (A) Fe_3O_4-NPs (n = 4); (B) Ag-NPs (n = 4) and (C) Fe_3O_4@Ag-NPs (n = 6). Data were expressed as mean ± standard error of mean (SEM). (*) Indicates a statistically significant difference in relation to the control group with $^*p < 0.05$, $^{****}p < 0.0001$ by One-way ANOVA followed by Tukey's comparisons test.

performed.

2.8. Egg laying and egg production assays

The egg laying was used to evaluate Fe_3O_4@Ag-NPs modulation of the cholinergic signaling in the N2 strain. 72 h after the end of exposure to hybrid NPs (first adult day), 2 worms from each group were transferred to NGM plates with or without the cholinergic agonist levamisole (500 mM). After 1 h, we measured the number of eggs laid by the worms on the plate and compared with the control group.

The egg production is used to assess the egg production capacity of worms. 72 h after the end of exposure to Fe_3O_4@Ag-NPs (first adult day), 5 worms of the N2 strain were exposed to a lysis solution (NaOH 1M, NaClO 1%, and distilled H_2O) under a glass slide. After the cuticle was broken, the number of eggs that were inside the worms was scored using a stereomicroscope (Leica S8 Apo Stereomicroscope, SP, Brazil) and compared with the control group. All assays were repeated at least three times.

2.9. Germline apoptosis

MD701 transgenic worms, which express the pro-apoptotic caspase CED-1 tagged with GFP, were exposed at the L4 stage to Fe_3O_4@Ag-NPs for 30 min and 24 h later (first adult day) they were collected with distilled water in microtubes and washed 3 times with distilled water after natural sedimentation. Then, the worms were transferred to glass slides containing levamisole (1 mM) and covered with coverslips to obtain images using the FLoid™ Cell Imaging Station fluorescent microscope (Thermo Fisher Scientific, Catalog number: 4471136, USA). The number of apoptotic germ cells was scored in both gonad arms and compared with the control group. 5 nematodes from each group were assessed in each one of the three independent experiments.

2.10. Swimming assay

Ten N2 worms per group treated at L1 stage to the treatments were transferred to plates containing 2 mL of M9 buffer (0.02 M KH_2PO_4, 0.04 M Na_2HPO_4 and 0.085 M NaCl) and habituated to the new environment for 1 min. Subsequently, the swimming movements were recorded in a stereomicroscope (Leica S8 Apo Stereomicroscope, SP, Brazil) and the videos analyzed using Image J (NIH, Bethesda, MD, USA) software for Windows with Worm Tracker plugin. We measured the velocity (mm/s) and distance (mm) travelled by the worms in the liquid medium for 1 min and compared with the control group. Assays were performed in three independent experiments.

2.11. Assessment of cholinergic and dopaminergic neurons

LX929 and BY200 worms were exposed to Fe_3O_4@Ag-NPs at L1 stage as described above and were collected 48 h after exposure with distilled water in microtubes and washed 3 times with distilled water after natural sedimentation. Then, the worms were transferred to glass slides containing levamisole (1 mM) and covered with coverslips to obtain images using the FLoid™ Cell Imaging Station fluorescent microscope (Thermo Fisher Scientific, Catalog number: 4471136, USA). To verify the morphology of cholinergic neurons, 10 worms per concentration were evaluated and the number of worms that presented abnormal morphology (y-shaped, blebbing, branching) in the axons and dendrites of these neurons was scored and compared with the control group. To evaluate the viability of cholinergic and dopaminergic neurons present in the head, images of 5 worms per concentration were obtained and the area fluorescence intensity of these neurons was subsequently evaluated using the Image J (NIH, Bethesda, MD, USA) software for Windows (Singh et al, 2023). The mean head fluorescence area was normalized by mean head fluorescence area of control worms (percentage of control).

These assays were repeated in at least three independent experiments.

2.12. Reactive oxygen species assay

To detect the levels of reactive oxygen species (ROS), 48 h after exposure to Fe_3O_4@Ag-NPs approximately 1500 worms of the N2 strain were transferred to a solution containing 50 mM of 5(6)-carboxy-2′,7′-dichlorofluoroscein diacetate (carboxy-DCFH-DA, Sigma) a well-established probe to detect and quantify ROS (Eruslanov and Kusmartsev, 2010). Worms were incubated for 1 h at 20 °C protected from light. Excess dye was removed by washing the worms 3 times with distilled water. In parallel, 10 μL of H_2O_2 (100 mM) was added in control group in order to stimulate the formation of ROS and used as a positive control. For imaging, the worms were placed on a glass slides containing levamisole (1 mM) for anesthesia and images of 5 worms per group, per independent assay, were acquired. The fluorescence was observed using a FLoid™ Cell Imaging Station fluorescent microscope (Thermo Fisher Scientific, Catalog number: 4471136, USA) and the intensity was measured using Image J (NIH, Bethesda, MD, USA) software for Windows. The mean fluorescence area was normalized by mean fluorescence area of control worms (percentage of control). To quantify ROS formation, the same procedure described above was performed, however, the amount of ROS formed was measured in a fluorimeter and readings were obtained every 15 min for 1 h at 25 °C (SpectraMax M5 Series Multi-Mode Microplate Readers, Molecular Devices, USA), with excitation wavelengths of 488 nm and emission of 500–538 nm. The results were normalized to the levels of proteins present in the samples (Bradford, 1976) and compared with the control group. These assays were repeated in at least three independent experiments.

2.13. DAF-16 localization

DAF-16 transcription factor was verified using a strain in which the promoter gene of this protein is tagged with green fluorescent protein (GFP). This factor, when located in the cell nucleus, leads to the expression of detoxifying and antioxidant enzymes. TJ356 worms were exposed for 30 min to Fe_3O_4@Ag-NPs right after exposure (still at the L1 stage) and were evaluated. The worms were transferred to glass slides containing levamisole (1 mM) and covered with coverslips for imaging using the FLoid™ Cell Imaging Station fluorescent microscope (Thermo Fisher Scientific, Catalog number: 4471136, USA). Results were expressed as nuclear, intermediate or cytosolic. All assays were repeated three times independently, using 30 worms per group in each assay.

2.14. GST-4 and SOD-3 expression

To verify the target DAF-16 genes following exposure to Fe_3O_4@Ag-NPs, the expression of GST-4 (glutathione-s-transferase) and SOD-3 (superoxide dismutase-3) were evaluated by using strains which the promoter genes of these proteins are tagged with GFP. To evaluate GST-4, 48h after exposure to NPs, CL2166 worms were collected with water in microtubes and washed 3 times with filtered water after natural sedimentation. To evaluate SOD-3, CF1553 worms were exposed to NPs and then (still at the L1 stage) were analyzed. In both analyses, the worms were transferred to glass slides containing levamisole (1 mM) and covered with coverslips to obtain the images using the FLoid™ Cell Imaging Station fluorescent microscope (Thermo Fisher Scientific, Catalog number: 4471136, USA). The mean fluorescence area intensity was subsequently evaluated using the Image J (NIH, Bethesda, MD, USA) software for Windows. We performed three independent assays with 5 animals in each group, per independent assay.

2.15. Glutathione-S-transferase activity

Forty-eight (48) hours after exposure to Fe_3O_4@Ag-NPs, approximately 3000 worms of the N2 strain were collected with distilled water in microtubes and washed 3 times with distilled water after natural sedimentation. Samples were frozen and thawed 3 times and then sonicated using the Ultrassonic Processor (Ultraschallprozessor, UP100H, Germany) to obtain a homogenate (three 10-s pulses performed three times on ice). After centrifugation (for 10 min, at 7000 rotations per minute, under 4 °C), the supernatant was collected and mixed with potassium phosphate buffer (TFK 30 mM, pH 7,4) and distilled water and incubated at 25 °C for 2 min in a 96-well plate. Reduced glutathione (GSH 1 mM) was used as substrate and dinitrochlorobenzene (CDNB 1 mM) was used to induce the reaction. Enzyme activity was read at 340 nm in a spectrophotometer (SpectraMax M5 Series Multi-Mode Microplate Readers, Molecular Devices, USA), at 30-s intervals for 5 min. The results were normalized for the levels of proteins present in the homogenate (Bradford, 1976) and compared with the control group. These assays were repeated in least three independent experiments.

2.16. Statistical analysis

All experiments were performed in duplicate or triplicate and repeated at least three times in independent experiments. Data were expressed as mean ± standard error of mean (SEM), with $p < 0.05$ considered statistically significant. The normality of data distribution was confirmed by the Shapiro-Wilk test (all $ps > 0.05$). Statistical significance survival (Ag-NPs, Fe_3O_4@Ag-NPs and survival comparison of NPs), length (Fe_3O_4-NPs and Fe_3O_4@Ag-NPs), brood size, egg production, number of apoptotic cells, distance travelled, fluorescence of cholinergic and dopaminergic neurons, ROS levels, DAF-16 localization, GST-4 and SOD-3 expression and GST activity were analyzed by One-way ANOVA followed by Tukey's multiple comparison test. To analyze the egg laying we used Two-way ANOVA followed by Tukey's multiple comparison test. To analyze the survival (F_3O_4-NPs), length (Ag-NPs), velocity and number of worms with abnormal cholinergic neurons we used the nonparametric test Kruskal-Wallis followed by Dunn's multiple comparisons test. The values of F, P, mean, standard (std) deviation and std error of mean are described in detail in Tables S1–S7. LC_{50} was reported as logarithmic concentration (μM) using the percentage of dead worms. Statistical analyses were performed using Graph Pad Prism Version 8.0.1 (244) software.

3. Results

3.1. Nanoparticles synthesis

Ag-NPs (average (hydrodynamic size of 35 nm) were obtained by reduction of silver ions (Ag^+) by green tea extract and well characterized, as described in Rolim et al. (2019). Fe_3O_4@Ag-NPs (average hydrodynamic size of 143 nm) were obtained and characterized as reported before (Pieretti et al. 2019). Table 1 shows the hydrodynamic size, polydispersity index and zeta potential for the three synthesized NPs (Fe_3O_4-NPs, Ag-NPs and Fe_3O_4@Ag-NPs). In addition, Fig. 1S shows representative electron microscopy micrographs of the three NPs, which were in accordance with hydrodynamic parameters. As previously reported, in the hybrid Fe_3O_4@Ag-NPs, the Fe_3O_4 and Ag mass fractions in are in 87.1 wt% and 12.9 wt%, respectively (Pieretti et al. 2019).

Table 1
Hydrodynamic size (% of intensity), polydispersity index (PDI) and zeta potential (mV) of the synthesized NPs.

Nanoparticle	Hydrodynamic size (% intensity/nm)	Polydispersity index (PDI)	Zeta potential (mV)
Ag-NPs	34.7 ± 4.0	0.28 ± 0.01	-35.5 ± 3.32
Fe_3O_4-NPs	350.5 ± 40.1	0.54 ± 0.03	- 8.56 ± 1.00
Fe_3O_4@Ag-NPs	143.6 ± 11.7	0.46 ± 0.03	- 32.73 ± 0.31

3.2. Survival rate

Survival is one of the initial parameters to evaluate the toxicity of new substances in studies with *C. elegans* (Long et al. 2023). In order to find the lethal concentration of these NPs, we performed a concentration-response curve. It was not possible to find a LC_{50} (lethal concentration) for Fe_3O_4-NPs and Ag-NPs, since these NPs did not show significant toxicity to the worms at the concentrations tested (Fig. 1A and B). However, an LC_{50} = 236 μg mL^{-1} was determined for Fe_3O_4@Ag-NPs, which showed a significant lethality from 50 μg mL^{-1} (Fig. 1C, $p < 0.001$). The comparison between the three NPs shows that the hybrid NPs shows higher lethality for *C. elegans* in relation to the monometallic NPs (Fig. 1D, $p < 0.0001$). LD_{50} values were calculated from the experimental LC_{50} obtained for Fe_3O_4@Ag-NPs during lethality trials using the regression function described in ICCVAM (2006). The predicted LD_{50} value was 0.346 mg kg^{-1} for mammals.

3.3. Fe_3O_4-NPs and Fe_3O_4@Ag-NPs cause alteration in *C. elegans* reproduction but do not change the development of the worms

To verify whether NPs change other physiological parameters besides survival, we verified the brood size and the development of the worms. *C. elegans* exposed to Fe_3O_4-NPs presented a reduced progeny at the 50 μg mL^{-1} (Fig. 2A, $p < 0.05$). However, worms exposed to Ag-NPs showed no change in reproduction (Fig. 2B). When evaluating the worms exposed to hybrid NPs, it was possible to observe that they showed a decrease in progeny from 10 μg mL^{-1} (Fig. 2C, $p < 0.05$), even though worms did not show a reproductive delay (Figure S 3C). The body length of the nematodes was evaluated in order to verify whether exposure to NPs interferes with the development of the worms. None of the NPs tested caused any change in the body length of *C. elegans* when compared to the control, which indicates that no developmental delay occurred (Fig. S 3A, 3B and 3C).

3.4. Hybrid NPs decrease egg-laying induced by cholinergic agonist levamisole but do not alter egg-production

To verify the relationship between the reprotoxicity and the integrity of the cholinergic signaling we used the levamisole induced egg-laying test. A decrease in egg laying of worms exposed only to NPs from 1 μg mL^{-1} was observed ($p < 0.05$). The decrease in egg laying observed after exposure to 1 μg mL^{-1} and 10 μg mL^{-1} was reversed by exposure to levamisole ($p < 0.01$). However, worms exposed to 50 μg mL^{-1} of Fe_3O_4@Ag-NPs showed an impaired cholinergic response, reducing the number of eggs laid even after exposure to the cholinergic agonist (Fig. 3A, $p < 0.0001$). It can also be observed that the egg production was not altered after exposure to hybrid NPs (Fig. 3B), thus indicating that there is an impairment in the eggs release by muscles controlled by the cholinergic system.

3.5. Fe_3O_4@Ag-NPs induce germline apoptosis

The MD701 strain allows the visualization of apoptotic corpses of germline cells by marking the *ced-1* gene, a caspase involved in cell apoptosis (Kinchen et al. 2005). It was possible to quantify a significant increase in the number of apoptotic cells in the germline cells of worms treated with 10 μg mL^{-1} and 50 μg mL^{-1} of Fe_3O_4@Ag-NPs (Fig. 4A and B, $p < 0.05$).

3.6. Fe_3O_4@Ag-NPs decrease the swimming movement rate

In order to evaluate whether the treatment with the hybrid NPs affected the movement of *C. elegans*, we verified the velocity and distance travelled by the worms during swimming. Both the velocity ($p < 0.01$) and distance ($p < 0.001$) swam by the worms were decreased after exposure of 50 μg mL^{-1} (Fig. 5A and B).

3.7. Fe_3O_4@Ag-NPs induce damage in cholinergic neurons but do not affect the dopaminergic neurons

Since we have found evidences of cholinergic impairment in swimming assay and in egg-laying- induced by levamisole, we verified the integrity of cholinergic neurons using the GFP tagged LX929 strain. It was possible to detect a high number of abnormalities (y-shaped axons) in the cholinergic neurons (Fig. 6A and D, $p < 0.05$), as well as a decrease in their fluorescence after exposure to 10 μg mL^{-1} and 50 μg mL^{-1} of Fe_3O_4@Ag-NPs (Fig. 6B and E, $p < 0.05$). To observe if another group of neurons important for locomotion were also affected, we observed the integrity of dopaminergic neurons using the BY200 strain. We did not observe any change in dopaminergic neurons after exposure to Fe_3O_4@Ag-NPs (Fig. 6C and F).

3.8. Fe_3O_4@Ag-NPs increase ROS production

Because oxidative stress is a common mechanism of NPs toxicity, especially neuronal and reproductive (Ajdary et al. 2018), we evaluated ROS levels in order to verify the redox status following exposure to NPs. In both analysis, after exposure to 50 μg mL^{-1} of Fe_3O_4@Ag-NPs there was an increase in ROS production when compared to the control group (Fig. 7A and B, $p < 0.05$). In addition, there was no significant difference

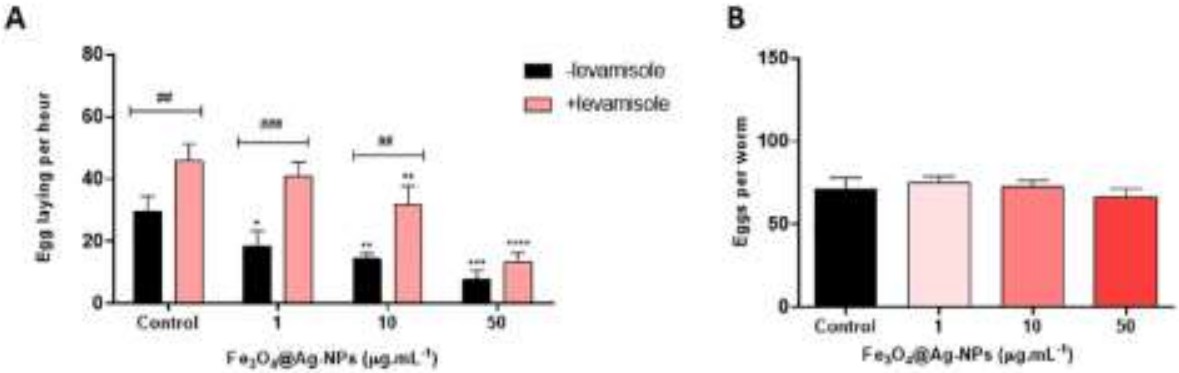

Fig. 3. Number of eggs laid decreased after exposure to Fe_3O_4@Ag-NPs, but egg production was not altered. In (A) is represented the egg-laying difference between worms with levamisole and without levamisole after exposure to Fe_3O_4@Ag-NPs in the first day adult (n = 4). Levamisole (500 mM) did not induced egg laying in worms exposed to 50 μg mL^{-1} of hybrid NPs. (#) Indicates statistically significant difference in relation to the (−) levamisole group with $^{\#\#}p < 0.01$, $^{\#\#\#}p < 0.001$, $^{\#\#\#\#}p < 0.0001$. (*) Denotes statistically significant difference in relation to control with $^{*}p < 0.05$, $^{**}p < 0.01$ by Two-way ANOVA followed by Tukey's multiple comparisons test. In (B) the egg production of the worms in the first day adult, analyzed by One-way ANOVA (n = 5). All data were expressed as mean ± standard error of mean (SEM).

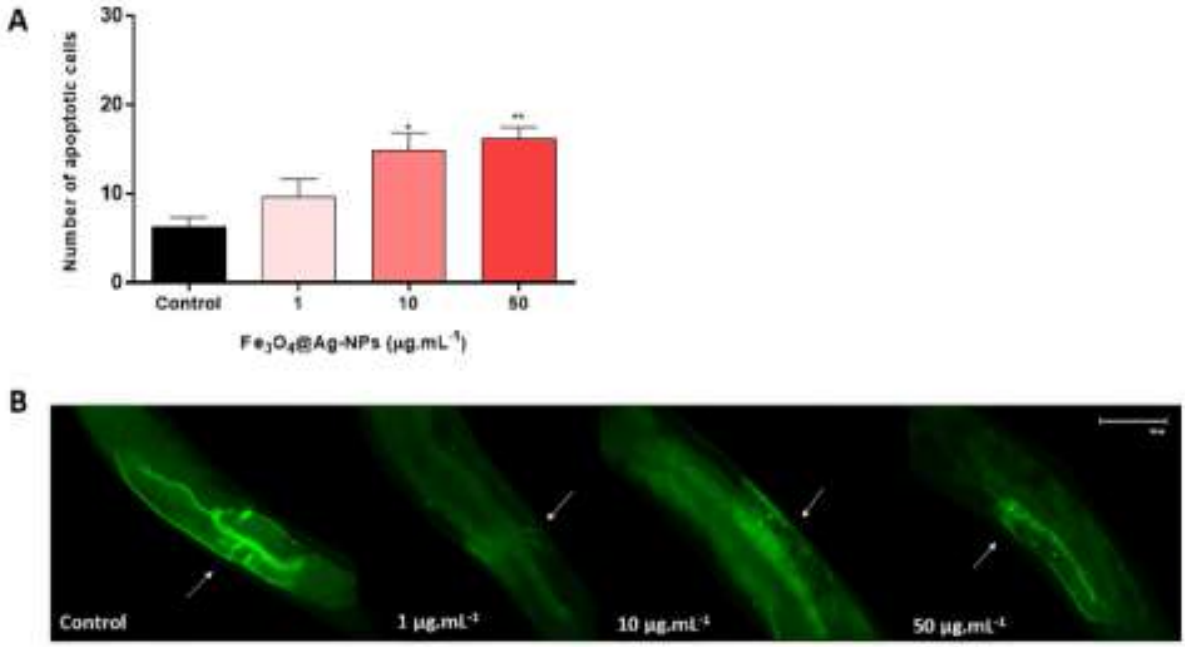

Fig. 4. Number of apoptotic cells increased after exposure to Fe_3O_4@Ag-NPs. (A) Number of apoptotic cells of worms in the first day adult (n = 4); (B) Representative images of MD701 strain showing apoptotic germline cells (indicated by arrows). Data were expressed as mean ± standard error of mean (SEM). (*) Indicates a statistically significant difference in relation to the control group with $^*p < 0.05$, $^{**}p < 0.01$ by One-way ANOVA followed by Tukey's multiple comparison test.

between worms exposed to positive control (H_2O_2) and the highest NPs concentration tested (Fig. 7A, B and 7C).

3.9. Fe_3O_4@Ag-NPs modulate transcription factor DAF-16

The migration of DAF-16 transcription factor from the cytosol to the cell nucleus is related to the activation of detoxifying enzymes in *C. elegans* (Murphy and Hu, 2013). We identified that DAF-16 migrated from the cytosol to the cell nucleus when worms were exposed to 10 μg mL^{-1} and 50 μg mL^{-1} of Fe_3O_4@Ag-NPs (Fig. 8A and B, $p < 0.01$).

3.10. Fe_3O_4@Ag-NPs increase the GST-4, SOD-3 expression and GST activity

To evaluate the antioxidant system of *C. elegans*, the protein expression of GST-4 and SOD-3 was verified (Fig. 9A and B). We observed an increase in GFP expression in both enzymes after exposure to 50 μg mL^{-1} of Fe_3O_4@Ag-NPs (Fig. 9C and D, $p < 0.05$). In addition, the activity of the glutathione-S-transferase, an enzyme involved in the cellular detoxification process of xenobiotics (Farina and Aschner, 2019) was also increased after exposure to Fe_3O_4@Ag- NPs (Fig. 9E, $p < 0.05$).

4. Discussion

The increasing use of products obtained through nanotechnology makes necessary to assess their biosafety (Lovern et al. 2007; Farré et al. 2009). Green synthesized NPs have been developed with the aim of enabling more efficient and low-cost final products, seeking to optimize the synthesis, improve properties and applications, in addition to providing a lower environmental impact (Arruebo et al. 2007). However, the same properties that make nanomaterials attractive may also be responsible for the harmful effects on exposed organisms (Dhawan and Sharma, 2010). In this sense, we sought to evaluate the safety of Fe_3O_4@Ag-NPs in *C. elegans*, a promising experimental model for the evaluation of nanomaterials since I) it has several orthologous genes to humans, which favors the prediction of the findings; II) it has a short life cycle, enabling faster results and; III) its transparent body allows the *in vivo* labeling and visualization of proteins involved in antioxidant and detoxification processes (Handy et al. 2012; Wu et al. 2019). In the light of green chemistry, Fe_3O_4@Ag-NPs were obtained by a simple chemical reduction of Fe^{3+} and Fe^{2+} ions, in aqueous medium at room temperature, leading to the Fe_3O_4 NPs (core), which was coated with biogenically synthesized Ag-NPs (shell), obtained by green tea extract. We have previously reported the cytotoxicity against cancer cell lines, antibacterial and hemocompatibility effects of Fe_3O_4@Ag-NPs (Pieretti et al. 2019), suggesting that these NPs might find important biomedical applications at safe dosages. In this study, we observed that high concentrations of these NPs caused toxicological outcomes, including increased oxidative stress and increased stress response, which was not enough to counteract ROS- induced apoptosis-dependent reprotoxicity and cholinergic neurotoxicity. The decrease in the swimming movements and in egg-laying induced by cholinergic agonist levemisole is in accordance with the abnormalities and decreased fluorescence of the cholinergic neurons in the nematodes exposed to high levels of the hybrid NPs.

Initially, we observed that *C. elegans* acutely exposed to Fe_3O_4@Ag-NPs presented significantly reduced survival and reproduction rates at the highest concentrations tested (Figs. 1C and 2C). On the other hand, when worms were exposed to Fe_3O_4-NPs and Ag-NPs at the same concentrations, there was no significant mortality (Fig. 1A and B). In relation to reproduction, Fe_3O_4-NPs showed a significant decrease after exposure to 50 μg mL^{-1} (Fig. 2A). However, no change in reproduction was observed after exposure to Ag-NPs (Fig. 2B). The development of the worms was not affected by any of the NPs evaluated (Figs. S3A and 3B e 3C). The acute oral toxicity potential of chemicals is usually determined by the calculation of the median lethal dose (LD_{50}) that is the dose that is expected to kill 50% of the test population. This parameter is crucial for hazard and risk assessment purposes, since it helps the industry, regulatory agencies and the international community for the hazard classification and labelling of chemicals and test materials (ICCVAM, 2006; Fuentes et al. 2022). In this study, the mammalian LD_{50} value based on the experimental LC_{50} was 0.346 mg kg^{-1}. The LD_{50} value found in this study is lower than the values reported for rodents when exposed to Fe_3O_4 and Ag NPs individually (MANEEWATTANAPINYO et al. 2011;

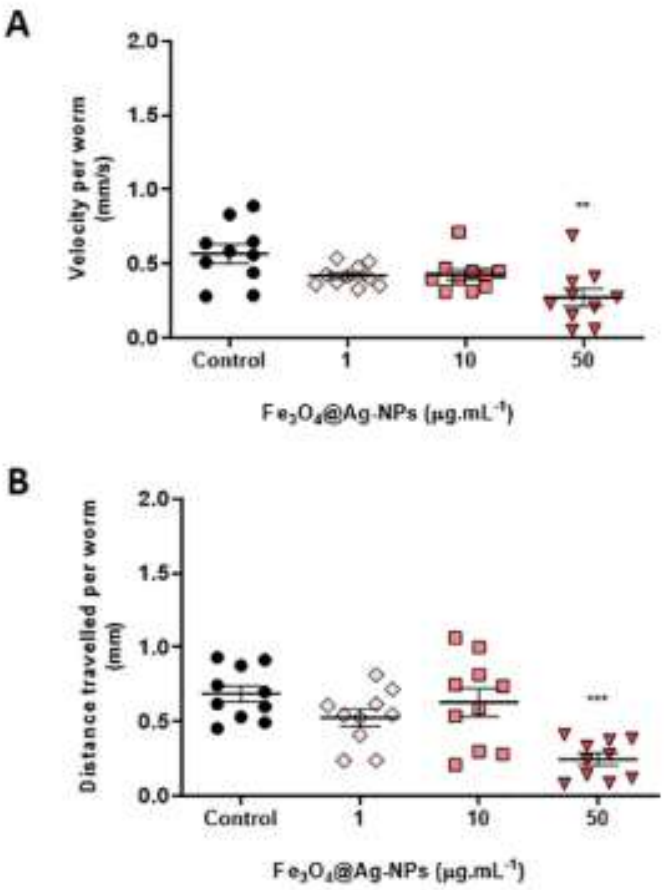

Fig. 5. Swimming movements decreased 48 h after exposure to Fe_3O_4@Ag-NPs. (A) Velocity and (B) distance travelled by the worms during the swimming assay (1 min; L4 stage) (n = 10). Data were expressed as mean ± standard error of mean (SEM). For the velocity analysis (*) indicates a statistically significant difference in relation to the control group with $^{**}p < 0.01$ by nonparametric Kruskal-Wallis test followed by Dunn's multiple comparison test. For the distance travelled analysis (*) denotes a statistically significant difference in relation to the control group with $^{**}p < 0.001$ by One-way ANOVA followed by Tukey's multiple comparison test.

Parivar et al. 2016), this can be justified because the existing results evaluate only isolated and non-hybrid NPs.

After observing that Fe_3O_4@Ag-NPs caused a decrease in brood size, indicating reproductive toxicity in *C. elegans*, we sought to evaluate more specific parameters. Cellular apoptosis may be related to reduced reproduction in *C. elegans*, as germline cells can undergo apoptosis due to DNA damage or oxidative stress (Jacques et al. 2019; Zečić and Braeckman, 2020). We verified an increase in the number of apoptotic cells in the nematode germline after exposure to the highest concentrations of Fe_3O_4@Ag-NPs (Fig. 4A e 4B), suggesting a cytotoxic effect, which was already observed in tumoral cell lines in the previous study using hybrid NPs (Pieretti et al., 2019). However, the apoptosis did not change the number of eggs inside the uterus (Fig. 3B), suggesting that the eggs produced may be infertile, since we observed reduced brood size. This data also suggested that eggs could be inside the uterus for a longer period of time in comparison to unexposed worms because of vulvar movements alterations. In order to observe whether the decrease in progeny size is related to the egg release by the vulva, we verified the number of eggs laid by nematodes after exposure to NPs. We observed that egg laying was also reduced in a concentration-dependent manner after treatment with hybrid NPs (Fig. 3A). To verify the possible involvement of the cholinergic system with this decrease in egg laying, we evaluated the exposure to the cholinergic agonist levamisole, which induces the egg release by increasing vulvar muscle contractions. Exposure to levamisole (500 mM) was able to induce egg laying in worms exposed to lower concentrations of NPs, however, the same did not occur after exposure to 50 µg mL^{-1} (Fig. 3A). These results suggest that besides activation of the apoptotic process, which reduces the generation of altered progeny, NPs exposure at high levels may be interfering with the cholinergic system, since it is directly involved in the mechanism of egg release through the vulva (Collins et al. 2016). Our hypothesis would be that cholinergic neurons may be undergoing cellular apoptosis as the germline cells, however, we do not have a strain that demonstrates this process exclusively in neurons, and therefore, we can only suggest that this process is occurring in neurons and other cells.

Once we observed significant reprotoxicity in the worms treated with higher concentrations of the hybrid NPs, we sought to elucidate the relationship of these effects with the cholinergic and dopaminergic system of *C. elegans*. It is known these systems are intimately involved in the control of worm muscles related to movement and egg release (Ikesmann et al. 2018; Ijomone et al. 2020). Thus, we evaluated the swimming movements and it was possible to observe a significant decrease in the velocity and distance travelled by the nematodes exposed to 50 µg mL^{-1} of Fe_3O_4@Ag-NPs (Fig. 5A and B). It is known that the vulvar muscles are excited rhythmically in conjunction with the body curves of nematodes. This is due to the signaling of cholinergic motor neurons, including the ventral C neurons (VCs), which are actived during locomotion (Weinshenker et al. 1995; Collins et al. 2016). A similar study by Marimon-Bolivar et al. (2019) with Fe_3O_4 magnetic nanoparticles (MNPs) in *C. elegans*, demonstrated that the presence of these nanomaterials increases mortality and decreases developmental parameters (size and egg laying), in addition to locomotor activity, suggesting a concentration-dependent effect (Marimon-Bolivar et al. 2019). In this sense, we evaluated the cholinergic neurons of the muscle and head of *C. elegans* and observed the formation of bifurcations (y-shaped) in the neurons present in the body (Fig. 6A and D), in addition to the decrease in the fluorescence of the neurons in the head (Fig. 6B and E). These results corroborate to the reproductive toxicity and the decreased swimming in the worms (Figs. 3A, 5A and 5B). Curiously, dopaminergic neurons were not affected in nematodes exposed to hybrid NPs (Fig. 6C and F). This could be due to a lower sensitivity of dopaminergic neurons to these NPs, or the different manner by which these NPs enter neurons. In addition, a study by Joshi demonstrated that *C. elegans* dopaminergic neurons promote proteostasis when exposed to a xenobiotic, increasing the expression of stress response genes (Joshi et al. 2016). One of the limitations of our study is that we did not evaluate the absorption of NPs in the systems separately, therefore, we cannot state whether these alterations are occurring by NPs differential absorption.

Previous studies have shown that chronic exposure to high concentrations of Ag-NPs promotes an increase in ROS formation (Soria et al. 2015; Singh et al. 2023) and activation of proteins involved in the stress response, including GST and SOD-3, as well as activation of cellular apoptosis and decrease in reproductive potential in *C. elegans* (Roh et al. 2009; Lim et al. 2012; Zečić and Braeckman, 2020). Therefore, we aimed to observe whether oxidative stress would be involved in toxic effects caused by high concentrations of Fe_3O_4@Ag-NPs. Using two methodologies, we observed that exposure to 50 µg mL^{-1} caused an increase in ROS levels compared to the control group, moreover, these levels were similar to those observed in the group exposed only to H_2O_2, used as a positive control (Fig. 7A, B and 7C). Following increase on ROS, the stress response in *C. elegans* is activated and controlled by several pathways, being the insulin/IGF-1-like/DAF-2 signaling pathway of major importance. The enzymes from the cascades have high structural and functional similarity to that of mammals and establish the interaction of nutrients with metabolism, in addition to being involved in the development, longevity, behavior and stress response in worms. The IIS/DAF-2 pathway is regulated by insulin-like ligands that bind to the mammalian DAF-2, ortholog of the transmembrane insulin receptor (IGFR)/IGF-1. DAF-2/IGFR controls the activity of a phosphoinositide

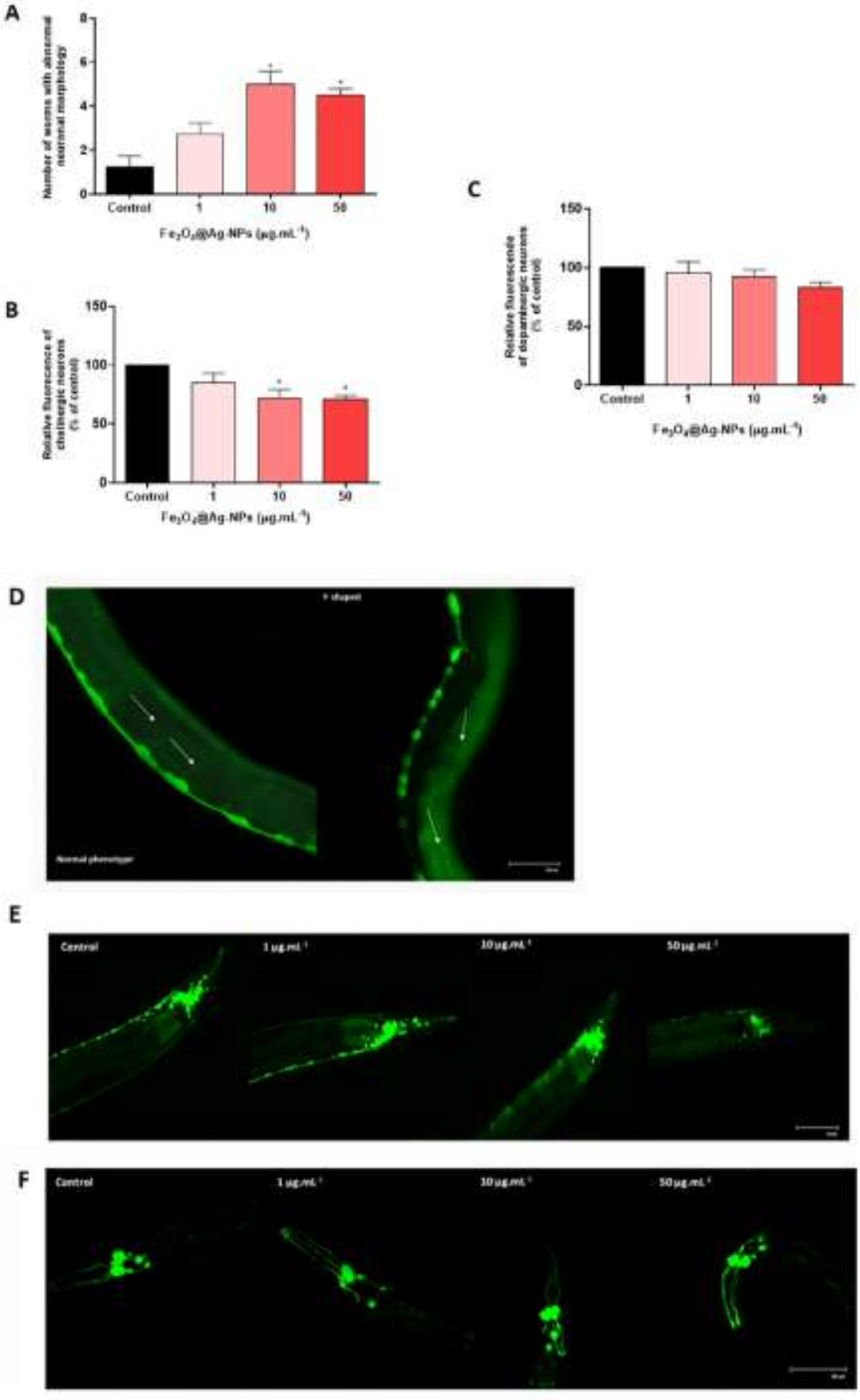

(caption on next page)

Fig. 6. Cholinergic neurons are affected following exposure to Fe_3O_4@Ag-NPs, however, dopaminergic neurons are not. (A) Number of abnormalities and (B) fluorescence intensity of cholinergic (n = 4) and (C) dopaminergic neurons (n = 3) (L4 stage). (D) Representative images of LX929 strain showing bifurcations (y-shaped) in cholinergic neurons (indicated by arrow) and (E) decreased fluorescence of cholinergic neurons in the head. (F) Representative images of dopaminergic neurons of BY200 strain exposed to Fe_3O_4@Ag-NPs. Data in A, B and C were expressed as mean ± standard error of mean (SEM). For the number of abnormalities analysis (*) indicates a statistically significant difference in relation to the control group with $^{*}p < 0.05$ by nonparametric Kruskal-Wallis test followed by Dunn's multiple comparison test. For the analysis of fluorescence intensity of cholinergic neurons (*) denotes a statistically significant difference in relation to the control group with $^{*}p < 0.05$ by One-way ANOVA followed by Tukey's multiple comparison test.

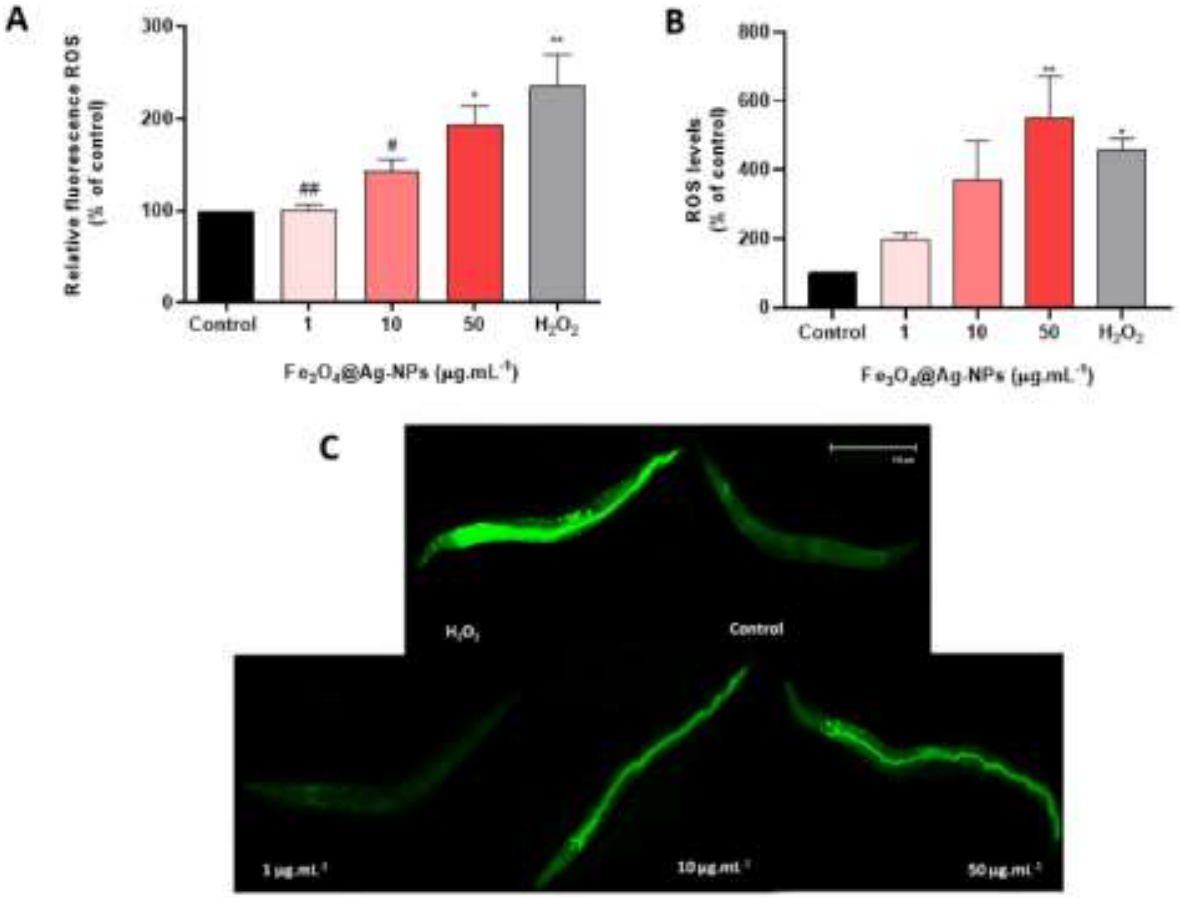

Fig. 7. ROS levels increased after the exposure to Fe_3O_4@Ag-NPs. (A) ROS levels measured by fluorescence imaging and (B) ROS levels measured in a fluorimeter (stage L4). (C) Representative images of ROS levels demonstrated in (A). Data were expressed as mean ± standard error of mean (SEM). (*) Denotes a statistically significant difference in relation to the control group with $^{*}p < 0.05$, $^{**}p < 0.01$. ($^{\#}$) Denotes a statistically significant difference in relation to the H_2O_2 group with $^{\#}p < 0.05$, $^{\#\#}p < 0.01$. Statistical analysis was performed by One-way ANOVA followed by Tukey multiple comparison test.

3-kinase (PI3K)/Akt kinase cascade, resulting in the regulation of transcription factor FOXO/DAF-16, which governs most of the functions of this pathway through migration from the cytoplasm to the nucleus, where it exerts its effects (Murphy and Hu, 2013; Sun et al. 2017; Rohn et al. 2018). One of the factors that induces this migration to the nucleus is the presence of ROS, aiming at activating the expression of enzymes such as GSTs and SODs that can protect the cells from external insults such as chemicals (Gurkar et al. 2018; Senchuk et al. 2018). We have found that hybrid NPs were able to promote the nuclear localization of DAF-16 (10 µg mL^{-1} and 50 µg mL^{-1}) (Fig. 8A and B). The activation of several subsequent proteins in these signaling cascades may indicate a defense mechanism of the organism against toxic agents (Blackwell et al. 2015; Tissenbaum, 2018). Previous studies have shown that toxic agents induce the nuclear localization of DAF-16 as an stress response (Ijomone et al. 2020; Ke et al. 2020).

To confirm this hypothesis, we evaluated the expression of the target genes GST-4 (stage L4) and SOD-3 (stage L1) tagged with GFP. The difference in the evaluation stage is due to the earlier response of SOD-3 expression against xenobiotics (Miao and St.Clair, 2009). Both expressions were increased after exposure to 50 µg mL^{-1} (Fig. 9A, B, 9D and 9E). Added to this, there was an increase in the enzymatic GST activity (Fig. 9F). These data reinforce the results obtained previously (Fig. 8A and B), where there was an increase in the translocation of DAF-16 to the cell nucleus, suggesting a detoxification mechanism in face of exposure to Fe_3O_4@Ag-NPs. The increase in the expression and activity of GST suggests a decrease in glutathione (GSH) levels, an antioxidant capable of mitigating the damage caused by ROS. Therefore, this decrease can make animals even more susceptible to oxidative stress, if they are not being replenished by a *de novo* synthesis of GSH (Nebert and Vasiliou, 2004; Canesi et al. 2010; Tu et al. 2010). The SOD-3 enzyme acts in the extracellular environment and catalyzes the dismutation of superoxide radical into oxygen and hydrogen peroxide, becoming an important antioxidant defense (Miao and St.Clair, 2009; Islam et al. 2021). The increase in this enzyme suggests an increase in ROS induced by toxicants, as depicted in this study (Fig. 7A, B and 7C).

In general, toxicological studies involving hybrid metallic nanoparticles are still scarce, making it difficult to estimate environmentally relevant environmental concentrations. In addition, there are few data

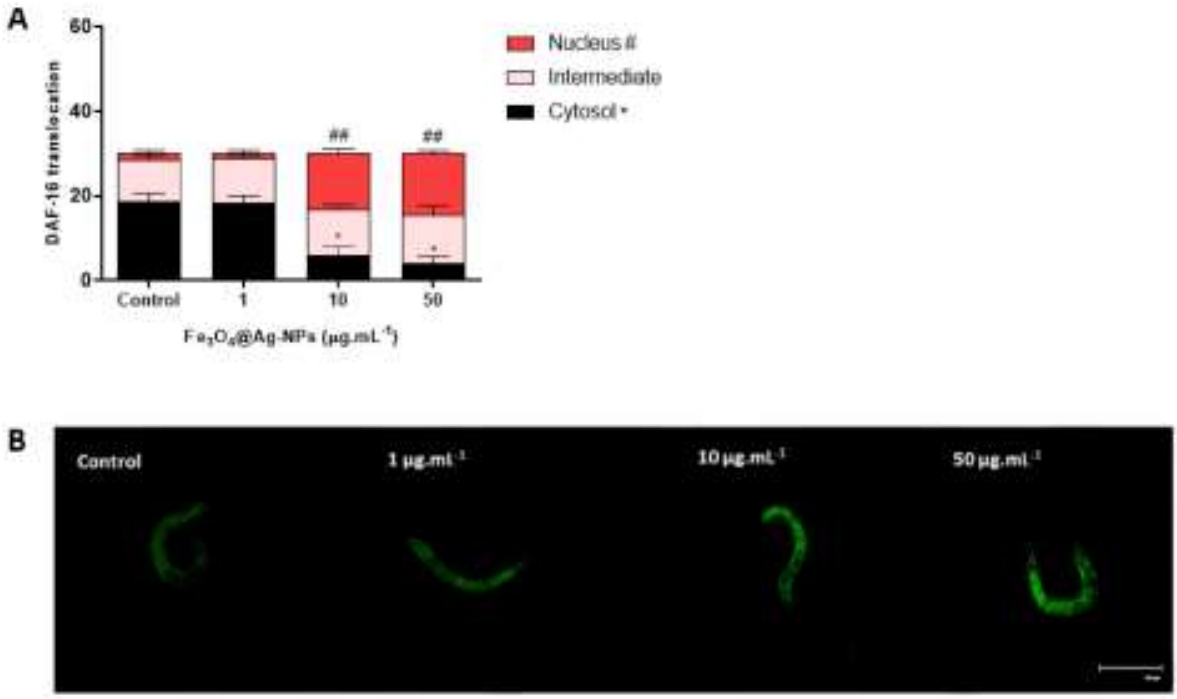

Fig. 8. Increased nuclear localization of DAF-16 after exposure to Fe_3O_4@Ag-NPs. (A) Cellular localization of the transcription factor *daf-16*::GFP in strain TJ356 (L1 stage) (n = 3) after exposure to Fe_3O_4@Ag-NPs. (B) Representatives of TJ356 strain exposed to Fe_3O_4@Ag-NPs. Data were expressed as mean ± standard error of mean (SEM). (*) Indicates a statistically significant difference from the number of cells in the cytosol with $^{*}p < 0.05$. (#) Denotes a statistically significant difference in the number of cells in the nucleus with $^{\#\#}p < 0.01$ by One-way ANOVA followed by Tukey's multiple comparison test.

that characterize the nanotoxicity of biogenic synthesized NPs, which makes it an area of great interest for further investigation. It is known that the toxicity of NPs is dependent on the absorption and retention of particles by the organism (Meyer et al. 2010), however, these parameters can be influenced by the chemical composition of the NPs, surface chemistry, which is related to the reactivity, as well as by the size of NPs, and state of agglomeration (Rossbach et al. 2020). Previous studies in cell culture show that the treatment using Fe_3O_4@Ag-NPs showed toxicity against tumor cell lineage (LC_{50} = 30 µg mL^{-1}) and also non-tumor cells (LC_{50} = 150 µg mL^{-1}), indicating a dose dependence in reducing cell viability (Pieretti et al. 2019). The synthesis of the NPs used in this study was performed by a simple co-precipitation of Fe^{2+}/Fe^{3+} in aqueous medium, in the absence of organic and toxic chemicals, followed by a biogenic reduction of Ag^{+} to Ag-NPs on the surface of Fe_3O_4-NPs, using *Camelia sinensis* (green tea) extract, since the use of plant extracts has great reducing potential due to the variety of molecules present in plants, such as polyphenols (Venkateswarlu et al. 2015), which prevent the oxidation and aggregation of NPs (Rolim et al. 2019). Because of these new characteristics and the increasing of use of nanomaterials in the biomedical area, it is relevant to analyze their effects and their potential toxicity preliminary in simpler organisms, in order to guarantee the safety of the applicability of these NPs.

5. Conclusion

In summary, it was possible to observe that, although synthesized using green chemistry, acute exposure to Fe_3O_4@Ag-NPs caused significant toxicity in nematodes at high tested concentrations. To the best of our knowledge, this is the first study to demonstrate the toxicity of these NPs *in vivo*. The results show that high levels of Fe_3O_4@Ag-NPs induce a decrease in worm survival and reproduction, observed through decreased brood size and egg laying. Reproductive toxicity seems to be related to germline cell apoptosis, oxidative stress and muscle cholinergic neuronal damage, impairing the release of vulvar eggs. The decrease in nematode swimming movements reinforces the hypothesis that the cholinergic system may be impaired, as the vulvar muscles are excited in conjunction with the body bends movement. Cholinergic damage may have been caused by oxidative stress, as increase in ROS levels and changes in stress response proteins were observed. The increased translocation of DAF-16 to the cell nucleus stands out, which corroborates with the greater expression and activity of GST, SOD-3 and increased cell apoptosis, as an indication of the activation of cellular detoxification mechanisms in *C. elegans*. These preliminary results suggest that these NPs are potentially toxic at high levels to *C. elegans* and although they show promising properties for biological applications, their levels should be monitored.

CRediT authorship contribution statement

Aline Castro Silva: The author participated in carrying out the experiments, in addition to writing, reviewing and organizing the research paper. **Alisson Gleysson Rodrigues dos Santos:** The author participated in carrying out the experiments, in addition to writing, reviewing and organizing the research paper. **Joana Claudio Pieretti:** The author participated in the synthesis and characterization of nanoparticles, in addition to writing, reviewing and organizing the research paper. **Wallace Rosado Rolim:** The author participated in the synthesis and characterization of nanoparticles, in addition to writing, reviewing and organizing the research paper. **Amedea Barozzi Seabra:** The author participated in the writing, revision, funding and organization of the research paper. **Daiana Silva Ávila:** The author participated in the writing, revision, funding and organization of the research paper.

Declaration of competing interest

The authors declare that they have no known competing financial interests or personal relationships that could have appeared to influence the work reported in this paper.

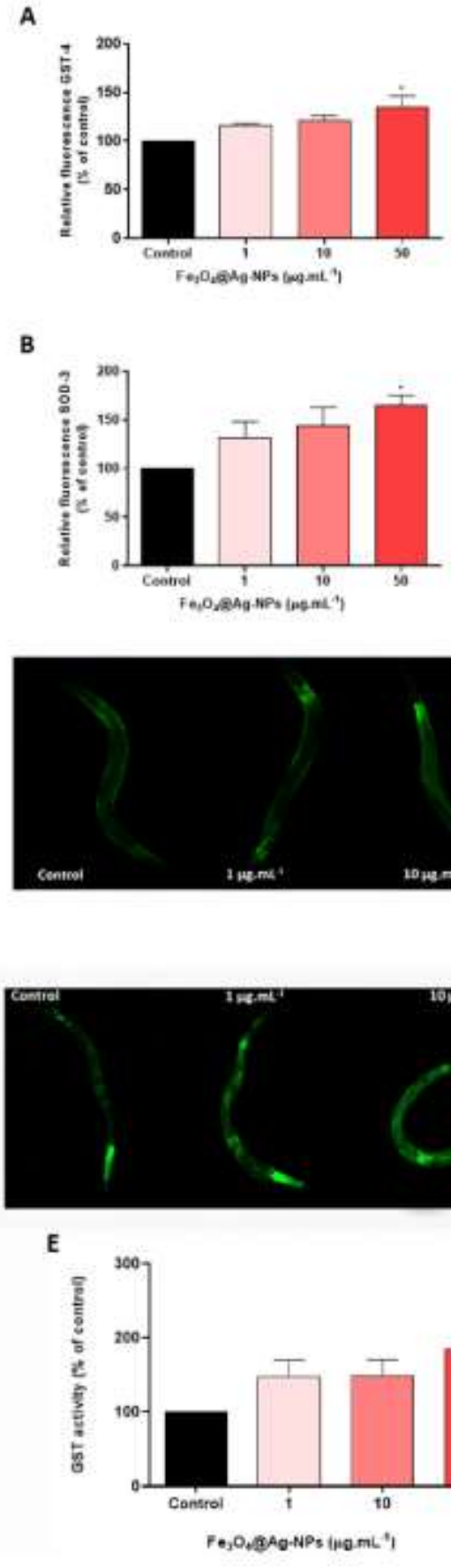

Fig. 9. Relative fluorescence of GST-4, SOD-3 and GST activity increased after exposure to Fe_3O_4@Ag-NPs. (A) Quantification of *gst-4*::GFP expression in strain CL2166 (L4 stage) (n = 3) and (B) *sod-3*::GFP in strain CF1553 (L1 stage) (n = 5) after exposure to Fe_3O_4@Ag-NPs. (C) Representative images of CL2166 and (D) CF1553 worms exposed to Fe_3O_4@Ag-NPs. (E) Quantification of GST enzyme activity after 48h exposure to Fe_3O_4@Ag-NPs (n = 5). Data were expressed as mean ± standard error of mean (SEM). (*) Denotes a statistically significant difference in relation to the control group with $^*p < 0.05$ by One-way ANOVA followed by Tukey's multiple comparisons test.

Data availability

Data will be made available on request.

Acknowledgements/Funding

The authors are thankful to Conselho Nacional de Desenvolvimento Científico e Tecnológico (CNPq-grants #301808/2018-0, #313117/2019-5, and scientific initiation schollarship for A.C.S), Universidade Federal do Pampa and Universidade Federal do ABC for funding and infra-structure, Fundação de Amparo à Pesquisa do Estado do Rio Grande do Sul (FAPERGS Grants #21/2551-0001963-8, #16/2551-0000248-7), Fundação de Amparo à Pesquisa do Estado de São Paulo (FAPESP, grants #2022/00321-0, 2020/03646-2), and scientific initiation schollarship for A.G.S.R), Coordenação de Aperfeiçoamento de Pessoal de Nível Superior (CAPES, Finance Code 001 for G.P.V and A.C.S).

Appendix A. Supplementary data

Supplementary data to this article can be found online at https://doi.org/10.1016/j.fct.2023.113945.

References

Ajdary, M., Moosavi, M., Rahmati, M., Falahati, M., Mahboubi, M., Mandegary, A., Jangjoo, S., Mohammadinejad, R., Varma, R., 2018. Health concerns of various nanoparticles: a review of their in vitro and in vivo toxicity. Nanomaterials 8 (9), 634.

Amigoni, L., Salvioni, L., Sciandrone, B., Giustra, M., Pacini, C., Tortora, P., Prosperi, D., Colombo, M., Regonesi, M.E., 2021. Impact of tuning the surface charge distribution on colloidal iron oxide nanoparticle toxicity investigated in Caenorhabditis elegans. Nanomaterials 11 (6), 1551.

Arruebo, M., Fernández-Pacheco, R., Ibarra, M.R., Santamaría, J., 2007. Magnetic nanoparticles for drug delivery. Nano Today 2 (3), 22–32.

Blackwell, T.K., Steinbaugh, M.J., Hourihan, J.M., Ewald, C.Y., Isik, M., 2015. SKN-1/Nrf, stress responses, and aging in Caenorhabditis elegans. Free Radic. Biol. Med. 88, 290–301.

Bury, A., Ho, H.K., 2020. All roads lead to the liver: metal nanoparticles and their implications for liver health. Small 16 (21), e2000153.

Bradford, M., 1976. A rapid and sensitive method for the quantitation of microgram quantities of protein utilizing the principle of protein-dye binding. Anal. Biochem. 72 (1–2), 248–254.

Bunluesl, A.-C., Gheraism, O., Grumezescu, A.M., Mogoantă, L., Fizaî, A., Andronescu, E., 2018. Biomedical applications of silver nanoparticles: an up-to-date overview. Nanomaterials 8 (9), 681.

Canesi, L., Fabbri, R., Gallo, G., Vallotto, D., Marcomini, A., Pojana, G., 2010. Biomarkers in Mytilus galloprovincialis exposed to suspensions of selected nanoparticles (Nano carbon black, C60 fullerene, Nano-TiO2, Nano-SiO2). Aquat. Toxicol. 100 (2), 168–177.

Collins, K.M., Bode, A., Fernandez, R.W., Tanis, J.E., Brewer, J.C., Creamer, M.S., Koelle, M.R., 2016. Activity of the C. elegans egg-laying behavior circuit is controlled by competing activation and feedback inhibition. Elife 5, e21126.

Dhawan, A., Sharma, V., 2010. Toxicity assessment of nanomaterials: methods and challenges. Anal. Bioanal. Chem. 398 (2), 589–605.

Durán, N., Rolim, W., Durán, M., Favaro, W., Seabra, A., 2018. NANOTOXICOLOGIA DE NANOPARTÍCULAS DE PRATA: TOXICIDADE EM ANIMAIS E HUMANOS. Química Nova, pp. 1–8. XX.

Ermakov, E., Kuznetsov, S., 2010. Identification of ROS using oxidized DCFDA and flow-cytometry. Methods Mol. Biol. 594, 57–72.

Essmann, C.L., Ryan, K.R., Elmi, M., Bryon-Dodd, E., Porter, A., Vaughan, A., McMullan, R., Nurrish, S., 2018. Activation of RHO-1 in cholinergic motor neurons competes with dopamine signalling to control locomotion. PLoS Gen. 13 (9), e0204057.

Farina, M., Aschner, M., 2019. Glutathione antioxidant system and methylmercury-induced neurotoxicity: an intriguing interplay. Biochim. Biophys. Acta Gen. Subj. 1863 (12), 129285.

Farré, M., Gajda-Schrantz, K., Kantiani, L., Barceló, D., 2009. Ecotoxicity and analysis of nanomaterials in the aquatic environment. Anal. Bioanal. Chem. 393 (1), 81–95.

Fuentes, C., Verdú, S., Fuentes, A., Ruiz, M.J., Barat, J.M., 2022. Effects of essential oil components exposure on biological parameters of Caenorhabditis elegans. Food Chem. Toxicol. 159, 112763.

Ghazanfari, M.R., Kashefi, M., Shams, S.F., Jaafari, M.R., 2016. Perspective of Fe3O4 nanoparticles role in biomedical applications. Biochemistry Research International 2016, 7840161.

Gurkar, A.U., Robinson, A.R., Cui, Y., Li, X., Allani, S.K., Webster, A., Muravia, M., Fallahi, M., Weinshach, H., Robbins, P.D., Wang, Y., Kelley, E.E., Cesic, C.M.S., Niedernhofer, L.J., Gill, M.S., 2018. Dysregulation of DAF-16/FOXO3A-mediated stress responses accelerates oxidative DNA damage induced aging. Redox Biol. 16, 191–199.

Handy, R.D., Cornelis, G., Fernandes, T., Tsyusko, O., Decho, A., Sabo-Attwood, T., Metcalfe, C., Steevens, J.A., Klaine, S.J., Koelmans, A.A., Horne, N., 2012. Ecotoxicity test methods for engineered nanomaterials: practical experiences and recommendations from the bench. Environ. Toxicol. Chem. 31 (1), 15–31.

Hussein Montazerian, A., Saber-Samandari, S., Khandan, A., 2018. Artificial intelligence investigation of three silicates bioceramics-magnetite bio-nanocomposite: hyperthermia and biomedical applications. Nano J. 5 (2), 163–171.

Ijomone, O.M., Miah, M.R., Akingbade, G.T., Bucinca, H., Aschner, M., 2020. Nickel-induced developmental neurotoxicity in C. elegans includes cholinergic, dopaminergic and GABAergic degeneration, altered behaviour, and increased SKN-1 activity. Neurotox. Res. 37 (4), 1018–1028.

Islam, M.N., Rauf, A., Fahad, F.I., Emran, T. Bin, Mitra, S., Olatunde, A., Shariati, M.A., Rebezov, M., Rengasamy, K.R.R., Mubarak, M.S., 2021. Superoxide dismutase: an updated review on its health benefits and industrial applications. Crit. Rev. Food Sci. Nutr. 61 (10), 1–19.

Jacques, M.T., Bunhout, J., Suarez, M.V., Schwerdtle, T., Garcia, S., Avila, D.S., 2019. Reprotoxicity of glyphosate-based formulation in Caenorhabditis elegans is not due to the active ingredient only. Environ. Pollut. 252 (Pt B), 1854–1862.

Joshi, K.K., Matlack, T.L., Rongo, C., 2016. Dopamine signaling promotes the xenobiotic stress response and protein homeostasis. EMBO J. 35 (17), 1885–1901.

Ke, T., Antunes Soares, F.A., Santamaría, A., Bowman, A.B., Skalny, A.V., Aschner, M., 2020. N,N' bis-(2-mercaptoethyl) isophthalamide induces developmental delay in Caenorhabditis elegans by promoting DAF-16 nuclear localization. Toxicol Rep 7, 930–937.

Kim, S.W., Nam, S.H., An, Y.J., 2012. Interaction of silver nanoparticles with biological surfaces of Caenorhabditis elegans. Ecotoxicol. Environ. Saf. 77, 64–70.

Kinchen, J.M., Cabello, J., Klingele, D., Wong, K., Feichtinger, R., Schnabel, H., Schnabel, R., Hengartner, M.O., 2005. Two pathways converge at CED-10 to mediate actin rearrangement and corpse removal in C. elegans. Nature 434 (7029), 93–99.

Lim, D., Roh, J.Y., Eom, H.J., Choi, J.Y., Hyun, J., Choi, J., 2012. Oxidative stress-related PMK-1 P38 MAPK activation as a mechanism for toxicity of silver nanoparticles to reproduction in the nematode Caenorhabditis elegans. Environ. Toxicol. Chem. 31 (3), 585–592.

Long, N.P., Kang, J.S., Kim, H.M., 2023. Caenorhabditis elegans: a model organism in the toxicity assessment of environmental pollutants. Environ. Sci. Pollut. Control Ser. 1–10, 2023.

Lovern, S.B., Strickler, J.R., Klaper, R., 2007. Behavioral and physiological changes in Daphnia magna when exposed to nanoparticle suspensions (titanium dioxide, nano-C60, and C 60HxC70Hx). Environ. Sci. Technol. 41 (12), 4465–4470.

Luo, X., Xu, S., Yang, Y., Li, L., Chen, S., Xu, A., Wu, L., 2016. Insights into the ecotoxicity of silver nanoparticles transferred from Escherichia coli to Caenorhabditis elegans. Sci. Rep. 6, 36465.

Maneewattanapinyo, P., Bandamara, W., Thammacharoen, C., Ekgasit, S., Kaewamatawong, T., 2011. An evaluation of acute toxicity of colloidal silver nanoparticles. J. Vet. Med. Sci. 73 (11), 1417–1423.

Marmolejo-Rodríguez, A.J., Durán-Domínguez-Arvizu, J.A., Tejeda-Benítez, L.P., Flores-Ávalos, C.A., De Leon-Rodríguez, D. De, 2019. Evaluation of the in vivo toxicity of green magnetic nanoparticles using Caenorhabditis elegans as a biological model. Environ. Nanotechnol. Monit. Manag. 12, 100253.

Meyer, J.N., Lord, C.A., Yang, X.Y., Turner, E.A., Badireddy, A.R., Marinakos, S.M., Chilkoti, A., Wiesner, M.R., Auffan, M., 2010. Intracellular uptake and associated toxicity of silver nanoparticles in Caenorhabditis elegans. Aquat. Toxicol. 100 (2), 140–150.

Miao, L., St Clair, D.K., 2009. Regulation of superoxide dismutase genes: implications in disease. Free Radic. Biol. Med. 47 (4), 344–356.

Montiel Schneider, M.G., Martín, M.J., Otarola, J., Vakarelska, E., Simeonov, V., Lassalle, V., Nedyalkova, M., 2022. Biomedical applications of iron oxide nanoparticles: current insights, progress and perspectives. Pharmaceutics 14 (1), 204.

Murphy, C.T., Hu, P.J., 2013. Insulin/insulin-like Growth Factor Signaling in C. elegans. Wormbook : the Online Review of C. elegans Biology, pp. 1–43.

Nebert, D.W., Vasiliou, V., 2004. Analysis of the glutathione S-transferase (GST) gene family. Hum. Genom. 1 (6), 460–464.

Pariyar, R., Mahdavand Fard, F., Bayat, M., Alavian, S.M., Motavaf, M., 2016. Evaluation of iron oxide nanoparticles toxicity on liver cells of BALB/c rats. Iran. Red Crescent Med. J. 18 (1), e28930.

Patiño-Ruiz, D., Sánchez-Botero, L., Tejeda-Benítez, L., Hinestroza, J., Herrera, A., 2020. Green synthesis of iron oxide nanoparticles using Cymbopogon citratus extract and sodium carbonate salt: nanotoxicological considerations for potential environmental applications. Environ. Nanotechnol. Monit. Manag. 14, 100377.

Pieretti, J.C., Beurton, J., Munevar, J., Nagamine, L.C.C.M., Le Faou, A., Seabra, A.B., Claeot, L., Boudier, A., 2021a. The impact of multiple functional layers in the structure of magnetic nanoparticles and their influence on albumin interaction. Int. J. Mol. Sci. 22 (19), 10477.

Pieretti, J.C., Gonçalves, M.C., Nakazato, G., Santos de Souza, A.C., Boudier, A., Seabra, A.B., 2021b. Multifunctional hybrid nanoplatform based on Fe3O4@Ag NPs for nitric oxide delivery: development, characterization, therapeutic efficacy, and hemocompatibility. J. Mater. Sci. Mater. Med. 32 (3), 23.

Pieretti, J.C., Rolim, W.R., Ferreira, F.F., Lombello, C.B., Nascimento, M.H.M., Seabra, A. B., 2019. Synthesis, characterization, and cytotoxicity of Fe3O4@Ag hybrid nanoparticles: promising applications in cancer treatment. J. Cluster Sci. 31 (2), 535–547.

Qu, M., Qiu, Y., Kong, Y., Wang, D., 2019. Amino modification enhances reproductive toxicity of nanopolystyrene on gonad development and reproductive capacity in nematode Caenorhabditis elegans. Environ. Pollut. 254, 112978.

Roh, J.Y., Sang, J.S., Yi, J., Park, K., Kyu, H.C., Ryu, D.Y., Choi, J., 2009. Ecotoxicity of silver nanoparticles on the soil nematode Caenorhabditis elegans using functional ecotoxicogenomics. Environ. Sci. Technol. 43 (10), 3923–3948.

Rohn, I., Marschall, T.A., Kroepfl, N., Jonen, K.B., Aschner, M., Tuck, S., Kuehnelt, D., Schwerdtle, T., Bornhorst, J., 2018. Selenium species-dependent toxicity, bioavailability and metabolic transformation in Caenorhabditis elegans. Metallomics 10 (6), 818–827.

Rollin, W.R., Pelegrino, M.T., de Araújo Lima, B., Ferraz, L.S., Costa, F.N., Bernardes, J. S., Rodigues, T., Brocchi, M., Seabra, A.B., 2019. Green tea extract mediated biogenic synthesis of silver nanoparticles: characterization, cytotoxicity evaluation and antibacterial activity. Appl. Surf. Sci. 463, 66–74.

Roubach, L.M., Oughton, D.H., Mazemnoti, E., Coutris, C., Brede, D.A., 2020. In vivo assessment of silver nanoparticle induced reactive oxygen species reveals tissue specific effects on cellular redox status in the nematode Caenorhabditis elegans. Sci. Total Environ. 721, 137965.

Senchuk, M.M., Dues, D.J., Schaar, C.E., Johnson, B.K., Madaj, Z.B., Bowman, M.J., Winn, M.E., Van Raamsdonk, J.M., 2018. Activation of DAF-16/FOXO by reactive oxygen species contributes to longevity in long-lived mitochondrial mutants in Caenorhabditis elegans. PLoS Genet. 14 (3), e1007268.

Singh, A.V., Chandrasekar, V., Paudel, N., Laux, P., Luch, A., Gemmati, D., Tisato, V., Prabhu, K.S., Uddin, S., Dakua, S.P., 2023. Integrative toxicogenomics: advancing precision medicine and toxicology through artificial intelligence and OMICs technology. Biomed. Pharmacother. 163, 114784.

Singh, A.V., Katz, A., Maharjan, R.S., Gadicherla, A.K., Richter, M.H., Heyda, J., del Pino, P., Laux, P., Luch, A., 2023. Coronavirus-mimicking nanoparticles (CorNPs) in artificial saliva droplets and nanoaerosols: influence of shape and environmental factors on particlokinetics/particle aerodynamics. Sci. Total Environ. 861, 160503.

Singh, K., Yadav, V.B., Yadav, U., Nath, G., Srivastava, A., Zamboni, P., Kerkar, P., Saxena, P.S., Singh, A.V., 2023. Evaluation of biogenic nanosilver-actieust for wound healing: a tri-modal in silico, in vitro and in vivo study. Colloids Surf. A Physicochem. Eng. Asp. 670, 131575.

Soria, C., Corrini, T., De Simone, U., Marchese, L., Zocatti, L., Giorgetti, S., Raimondi, S., Mangione, P.P., Ramat, S., Bellotti, V., Manzo, L., Stoppini, M., 2015. Enhanced toxicity of silver nanoparticles in transgenic Caenorhabditis elegans expressing amyloidogenic proteins. Amyloid 2 (4), 221–228.

Spagnoletti, F.N., Kronberg, F., Spedalieri, C., Munarriz, E., Giacometti, R., 2021. Protein corona on biogenic silver nanoparticles provides higher stability and protects cells from toxicity in comparison to chemical nanoparticles. J. Environ. Manag. 297, 113434.

Stiernagle, T., 2006. Maintenance of C. elegans. Worm 6, 51–67.

Sun, X., Chen, W.D., Wang, Y.D., 2017. DAF-16/FOXO transcription factor in aging and longevity. Front. Pharmacol. 8, 548.

Tejeda-Benitez, L., Olivero-Verbel, J., 2016. Caenorhabditis elegans, a biological model for research in toxicology. Rev. Environ. Contam. Toxicol. 237, 1–35.

Thasenbaum, H.A., 2018. DAF-16: FOXO in the Context of C. elegans, first ed., 127. Current Topics in Developmental Biology, Elsevier Inc, pp. 1–21.

Tu, H.T., Silvestre, F., Wang, N., Thome, J.P., Phuong, N.T., Kestemont, P., 2010. A multi-biomarker approach to assess the impact of farming systems on black tiger shrimp (Penaeus monodon). Chemosphere 81 (10), 1204–1211.

Venkateswarlu, S., Natesh Kumar, B., Prathima, B., Anitha, K., Jyothi, N.V.V., 2015. A novel green synthesis of Fe3O4-Ag core shell recyclable nanoparticles using Vitis vinifera stem extract and its enhanced antibacterial performance. Phys. B Condens. Matter 457, 30–35.

Weinshenker, D., Garriga, G., Thomas, J., 1995. Genetic and pharmacological analysis of neurotransmitters controlling egg laying in C. elegans. J. Neurosci. 15 (10), 6975–6985.

Wu, T., Xu, H., Liang, X., Tang, M., 2019. Caenorhabditis elegans as a complete model organism for biosafety assessments of nanoparticles. Chemosphere 221, 708–726.

Yang, Y.-F., Chen, P.-J., Liao, V.H.-C., 2016. Nanoscale zerovalent iron (nZVI) at environmentally relevant concentrations induced multigenerational reproductive toxicity in Caenorhabditis elegans. Chemosphere 150, 615–623.

Zečić, A., Braeckman, B.P., 2020. DAF-16/FoxO in Caenorhabditis elegans and its role in metabolic remodeling. Cells 9 (1), 109.

Supplementary Materials

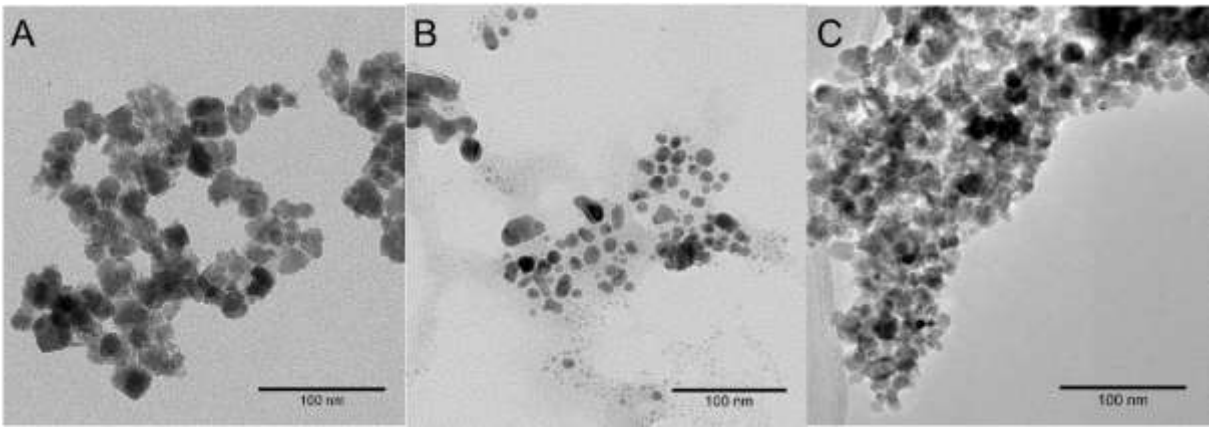

Figure 1S. Transmission electron microscopy micrographs of (A) Fe_3O_4@Ag-NPs, (B) Ag-NPs and (C) Fe_3O_4@Ag-NPs.

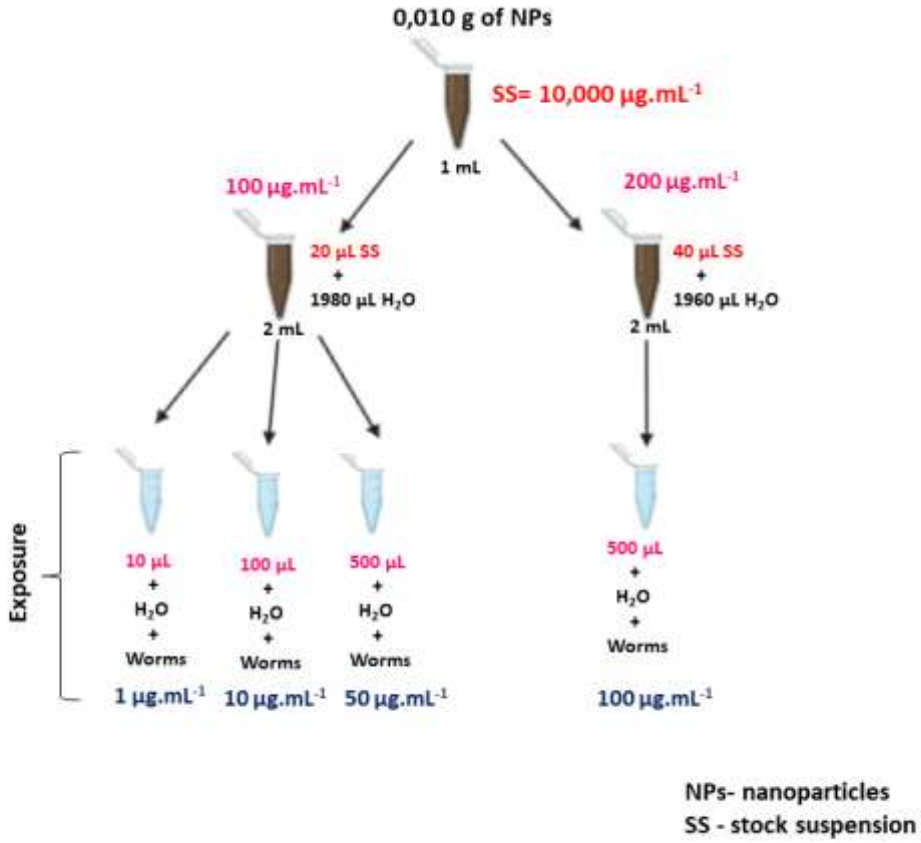

Figure 2S. Representative image of the preparation of stock suspensions of Fe_3O_4, Ag and

Fe_3O_4@Ag nanoparticles. **NPs=** nanoparticles; **SS=**stock suspension.

Table 1S. Description of the parametric statistical analysis by one-way ANOVA followed by Tukey's comparisons test.

Analyzed Parameters	**F (DFn, DFd)**	**P value**
Body length - Fe_3O_4-NPs	1.018 (4, 17)	0.4260
Body length - Fe_3O_4@Ag-NPs	1.573 (4, 20)	0.2200
Brood size - Fe_3O_4-NPs	3.751 (4, 14)	0.0282
Brood size - Ag-NPs	0.801 (4, 15)	0.5429
Brood size - Fe_3O_4@Ag-NPs	15.560 (4, 23)	<0.0001
Fluorescence intensity of cholinergic neurons	5.484 (3, 12)	0.0132
DAF-16 localization	15.340 (11, 24)	<0.0001
Distance travelled	8.908 (3, 36)	0.0002
Dopaminergic neurons	1.411 (3, 8)	0.3091
Germline apoptosis	7.707 (3, 12)	0.0039
Glutathione-S-transferase activity	4.213 (3, 20)	0.0183
GST-4 expression	4.933 (3, 8)	0.0316
Number of eggs	0.447 (3, 16)	0.7225
Reactive oxygen species (images)	2.293 (4, 15)	0.1073
Reactive oxygen specie	3.706 (4, 15)	0.0273
SOD-3 expression	3.852 (3, 12)	0.0384
Survival comparison	10.520 (14, 56)	<0.0001
Survival rate – Ag-NPs	0.573 (4, 10)	0.6885
Survival rate – Fe_3O_4@Ag-NPs	13.660 (4, 22)	<0.0001

Table 2S. Description of the parametric statistical analysis by two-way ANOVA followed by Tukey's comparisons test.

Analyzed Parameters	**F (DFn, DFd)**	**P value**
Egg laying	6.663 (3, 9)	0.0116

Table 3S. Description of nonparametric statistical analysis by Kruskal-Wallis test followed by Dunn's comparisons test.

Analyzed Parameters	**Kruskal-Wallis statistic**	**P value**
Abnormal morphology of cholinergic neurons	11.640	0.0004
Body length - Ag-NPs	2.807	0.5907
Survival - Fe_3O_4-NPs	3.937	0.4146
Velocity	12.360	0.0063

Table 4S. Description of the mean, standard (std) deviation and std error of mean of analyzes performed.

Analyzed Parameters	Control			1 µg.mL^{-1}			10 µg.mL^{-1}			50 µg.mL^{-1}			100 µg.mL^{-1}		
	Mean	**Std Deviation**	**Std Error of Mean**	**Mean**	**Std Deviation**	**Std Error of Mean**	**Mean**	**Std Deviation**	**Std Error of Mean**	**Mean**	**Std Deviation**	**Std Error of Mean**	**Mean**	**Std Deviation**	**Std Error of Mean**
Abnormal morphology of cholinergic neurons	1.2	0.9	0.4	2.7	0.0	0.4	5.0	1.0	0.5	4.5	0.5	0.2	-	-	-
Body length - Ag-NPs	100.0	0.0	0.0	104.2	12.0	6.0	99.0	2.0	1.0	103.7	7.3	3.6	104.9	26.2	13.1
Body length - Fe_3O_4@Ag-NPs	100.0	0.0	0.0	97.5	10.0	3.8	93.8	12.1	5.4	96.6	14.9	8.6	82.8	15.4	8.9
Body length - Fe_3O_4-NPs	100.0	0.0	0.0	97.8	12.2	5.0	99.4	4.6	2.3	93.1	11.5	6.6	90.0	5.4	3.1
Brood size - Ag-NPs	100.0	0.0	0.0	105.2	5.3	0.2	103.8	8.2	4.1	102.4	14.4	7.2	116.8	27.4	13.7
Brood size - Fe_3O_4@Ag-NPs	100.0	0.0	0.0	86.8	7.0	2.8	80.0	12.4	5.0	52.3	19.1	8.5	61.0	11.4	5.1
Brood size - Fe_3O_4-NPs	100.0	0.0	0.0	78.7	10.3	5.1	75.7	13.9	6.9	67.4	9.8	4.9	72.3	23.5	13.6
Distance travelled	0.6	0.1	0.0	0.5	0.1	0.0	0.6	0.2	0.0	0.2	0.1	0.0	-	-	-
Dopaminergic neurons	100.0	0.0	0.0	95.6	16.3	9.4	92.2	10.3	5.9	83.3	7.1	4.1	-	-	-
Fluorescence intensity of	100.0	0.0	0.0	84.8	16.9	8.4	72.	14.5	7.2	71.2	5.5	2.7	-	-	-

cholinergic neurons															
Germline apoptosis	6.3	1.9	0.9	9.5	4.2	2.1	14.9	3.7	1.8	16.1	2.7	1.3	-	-	-
Glutathione-S-transferase activity	100.0	0.0	0.0	147.4	54.3	22.1	149.4	51.5	21.0	185.0	36.2	14.7	-	-	-
GST-4 expression	100.0	0.0	0.0	116.1	3.0	1.7	121.5	7.9	4.5	134.5	20.5	11.8	-	-	-
Number of eggs	71.2	16.0	7.1	74.8	9.2	4.1	72.6	8.5	3.8	66.6	10.9	4.9	-	-	-
Reactive oxygen species	100.0	0.0	0.0	197.1	36.0	18.0	370.5	229.0	114.5	550.8	243.3	121.7	-	-	-
Reactive oxygen species (images)	100.0	0.0	0.0	100.8	11.2	5.62	143.8	22.7	11.3	193.0	41.2	20.6	-	-	-
SOD-3 expression	100.0	0.0	0.0	131.8	33.1	16.5	143.7	38.9	19.4	165.0	21.0	10.5	-	-	-
Survival - Fe_3O_4-NPs	100.0	0.0	0.0	101.3	7.0	2.8	96.5	10.3	4.2	94.6	9.0	3.6	-	-	-
Survival rate – Ag-NPs	100.0	0.0	0.0	102.9	4.9	2.8	95.6	2.8	1.6	109.9	24.5	14.1	98.8	11.4	6.5
Survival rate – Fe_3O_4@Ag-NPs	100.0	0.0	0.0	93.0	14.1	5.7	80.6	14.7	6.0	61.1	14.3	6.4	56.2	5.3	2.6
Velocity	0.5	0.2	0.0	0.4	0.0	0.0	0.4	0.1	0.0	0.2	0.1	0.0	-	-	-

Table 5S. Description of the mean, standard (std) deviation and std error of mean of survival comparison.

Survival comparison								
Control								
Mean			Std Deviation			Std Error of Mean		
Hybrid NPs	Fe_3O_4@Ag-NPs	Ag-NPs	Hybrid NPs	Fe_3O_4@Ag-NPs	Ag-NPs	Hybrid NPs	Fe_3O_4@Ag-NPs	Ag-NPs
100.0	100.0	100.0	0.0	0.0	0.0	0.0	0.0	0.0
1 µg.mL^{-1}								
Mean			Std Deviation			Std Error of Mean		
Hybrid NPs	Fe_3O_4@Ag-NPs	Ag-NPs	Hybrid NPs	Fe_3O_4@Ag-NPs	Ag-NPs	Hybrid NPs	Fe_3O_4@Ag-NPs	Ag-NPs
93.1	101.3	102.9	14.2	7.0	4.9	5.7	2.8	2.8
10 µg.mL^{-1}								
Mean			Std Deviation			Std Error of Mean		
Hybrid NPs	Fe_3O_4@Ag-NPs	Ag-NPs	Hybrid NPs	Fe_3O_4@Ag-NPs	Ag-NPs	Hybrid NPs	Fe_3O_4@Ag-NPs	Ag-NPs
80.6	96.5	95.6	14.7	10.3	2.8	6.0	4.2	1.6
50 µg.mL^{-1}								
Mean			Std Deviation			Std Error of Mean		
Hybrid NPs	Fe_3O_4@Ag-NPs	Ag-NPs	Hybrid NPs	Fe_3O_4@Ag-NPs	Ag-NPs	Hybrid NPs	Fe_3O_4@Ag-NPs	Ag-NPs
61.1	94.6	100.5	14.3	9.0	8.3	6.4	3.6	4.7
100 µg.mL^{-1}								
Mean			Std Deviation			Std Error of Mean		
Hybrid NPs	Fe_3O_4@Ag-NPs	Ag-NPs	Hybrid NPs	Fe_3O_4@Ag-NPs	Ag-NPs	Hybrid NPs	Fe_3O_4@Ag-NPs	Ag-NPs
56.2	103.8	98.8	5.3	11.8	11.4	2.6	5.2	6.5

Table 6S. Description of the mean, standard (std) deviation and std error of mean of egg laying.

Egg laying					
Control					
Mean		Std Deviation		Std Error of Mean	
(-) levamisole	(+) levamisole	(-) levamisole	(+) levamisole	(-) levamisole	(+) levamisole
29.7	45.7	9.6	10.9	4.8	5.4
1 µg.mL^{-1}					
Mean		Std Deviation		Std Error of Mean	
(-) levamisole	(+) levamisole	(-) levamisole	(+) levamisole	(-) levamisole	(+) levamisole
18.5	41.0	9.9	9.0	4.9	4.5
10 µg.mL^{-1}					
Mean		Std Deviation		Std Error of Mean	
(-) levamisole	(+) levamisole	(-) levamisole	(+) levamisole	(-) levamisole	(+) levamisole
14.5	31.7	3.3	12.0	1.6	6.0
50 µg.mL^{-1}					
Mean		Std Deviation		Std Error of Mean	
(-) levamisole	(+) levamisole	(-) levamisole	(+) levamisole	(-) levamisole	(+) levamisole
7.7	13.2	6.0	6.2	3.0	3.1

Table 7S. Description of the mean, standard (std) deviation and std error of mean of DAF-16 translocation.

DAF-16 translocation								
Control								
Cytosol			Intermediate			Nucleus		
Mean	Std Deviation	Std Error of Mean	Mean	Std Deviation	Std Error of Mean	Mean	Std Deviation	Std Error of Mean
18.6	3.2	1.8	9.6	2.0	1.2	1.6	1.5	0.8
1 µg.mL^{-1}								
Cytosol			Intermediate			Nucleus		
Mean	Std Deviation	Std Error of Mean	Mean	Std Deviation	Std Error of Mean	Mean	Std Deviation	Std Error of Mean
18.3	3.0	1.7	10.3	1.5	0.8	1.3	1.5	0.8
10 µg.mL^{-1}								
Cytosol			Intermediate			Nucleus		
Mean	Std Deviation	Std Error of Mean	Mean	Std Deviation	Std Error of Mean	Mean	Std Deviation	Std Error of Mean
6.0	3.6	2.0	10.3	2.5	1.4	13.3	2.0	1.2
50 µg.mL^{-1}								
Cytosol			Intermediate			Nucleus		
Mean	Std Deviation	Std Error of Mean	Mean	Std Deviation	Std Error of Mean	Mean	Std Deviation	Std Error of Mean
4.0	3.0	1.7	11.3	4.0	2.3	14.6	1.5	0.8

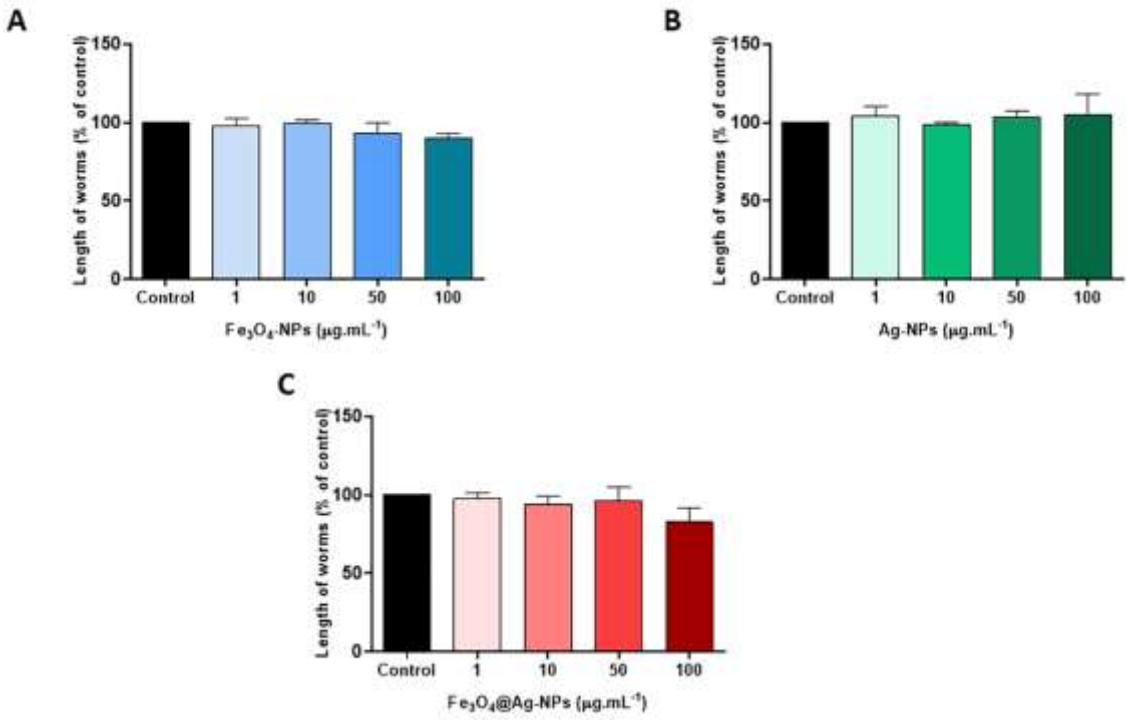

Figure 3S. Exposure to NPs did not alter the body length. Body length of worms exposed to different concentrations of (A) Fe_3O_4-NPs (n=6); (B) Ag-NPs (n=4) and (C) Fe_3O_4@Ag-NPs (n=7) (L4 stage). Data were expressed as mean ± standard error of mean (SEM). The analysis of the body length for Fe_3O_4-NPs and Fe_3O_4@Ag-NPs was performed by One-way ANOVA. To analyze of the body length of worms exposed to Ag-NPs was performed by nonparametric Kruskal-Wallis test.

6. CONSIDERAÇÕES FINAIS

O aumento do uso de produtos obtidos por meio da nanotecnologia gera a necessidade da ampliação de estudos sobre a segurança dessas substâncias. Nanopartículas híbridas representam uma promissora estratégia no desenvolvimento de nanomateriais versáteis com diferentes características e funções em uma única nanoestrutura. No entanto, existem poucos estudos *in vivo* que comprovem a segurança de Fe_3O_4@Ag-NPs sintetizadas por rota biogênica, sendo necessárias

maiores investigações sobre sua atuação em sistemas biológicos.

As Fe_3O_4@Ag-NPs apresentaram toxicidade significativa na sobrevivência e reprodução de *C. elegans,* todavia o mesmo não ocorreu para Fe_3O_4-NPs e Ag-NPs. Além disso, a exposição a Fe_3O_4@Ag-NPs diminuiu a postura de ovos, bem como causou o aumento da apoptose celular na linhagem germinativa dos vermes. Após a exposição ao agonista colinérgico levamisol, a postura de ovos não foi estimulada na maior concentração testada, sugerindo que a toxicidade está relacionada com o sistema colinérgico.

De forma geral, é possível verificar que Fe_3O_4@Ag-NPs causam toxicidade significativa em *C. elegans.* Nosso trabalho sugere que o mecanismo de toxicidade das Fe_3O_4@Ag-NPs atua no sistema colinérgico diminuindo a reprodução e o movimento natatório dos vermes, ativando também a apoptose celular. Além disso, observamos o aumento dos níveis de EROs e a modulação do fator de transcrição DAF-16, por meio da sua translocação para o núcleo celular e consequentemente a ativação de processos de detoxificação, verificados pelo aumento da expressão de GST-4, SOD-3 e atividade de GST.

7. REFERENCIAS

ARRUEBO, M. *et al.* Magnetic nanoparticles for drug delivery. Nano Today, [*s. l.*], v. 2, n. 3, p. 22–32, 2007.

ARVANITIS, M. *et al.* Apoptosis in c.elegans: Lessons for cancer and immunity. Frontiers in Cellular and Infection Microbiology, [*s. l.*], v. 3, p. 67, 2013.

BAEZA, A.; GUILLENA, G.; RAMÓN, D. J. Magnetite and Metal-Impregnated Magnetite Catalysts in Organic Synthesis: A Very Old Concept with New Promising Perspectives. [*S. l.: s. n.*], v. 8, n.1, p. 49-67, 2016.

BAI, C.; TANG, M. Toxicological study of metal and metal oxide nanoparticles in zebrafish. [*S. l.: s. n.*], v. 40, n. 1, p. 37-63, 2020.

BOEY, A.; HO, H. K. All Roads Lead to the Liver: Metal Nanoparticles and Their Implications for Liver Health. [*S. l.: s. n.*], v.16, n. 21, p. e2000153, 2020.

COLLINS, K. M. *et al.* Activity of the C. elegans egg-laying behavior circuit is controlled by

competing activation and feedback inhibition. eLife, [*s. l.*], v.5, p. e21126, 2016.
CORSI, Ann K; WIGHTMAN, B.; CHALFIE, M. A Transparent Window into Biology: A Primer on *Caenorhabditis elegans*. Genetics, [*s. l.*], v. 200, n. 2, p. 387–407, 2015.
CULETTO, E. A role for Caenorhabditis elegans in understanding the function and interactions of human disease genes. Human Molecular Genetics, [*s. l.*], v. 9, n. 6, p. 869-77, 2000.
DURÁN, N. *et al.* NANOTOXICOLOGIA DE NANOPARTÍCULAS DE PRATA: TOXICIDADE EM ANIMAIS E HUMANOS. Química Nova, [*s. l.*], v. XY, p. 1–8, 2018.
EMBRY, M. R. *et al.* The fish embryo toxicity test as an animal alternative method in hazard and risk assessment and scientific research. [*S. l.: s. n.*], v. 97, n. 2., p. 79-87, 2010.
EMERSON, S. *et al.* Acetylcholine signaling genes are required for cocaine-stimulated egg laying in *Caenorhabditis elegans*. G3 Genes|Genomes|Genetics, [*s. l.*], v. 11, n. 8, 2021.
FAGAN, K. A.; PORTMAN, D. S. Sexual modulation of neural circuits and behavior in Caenorhabditis elegans. Seminars in Cell & Developmental Biology, [*s. l.*], v. 33, p. 3–9, 2014.
GARTNER, A.; BOAG, P. R.; BLACKWELL, T. K. Germline survival and apoptosis. [*S. l.: s. n.*], v.08, p. 1-20, 2008.
GHAZANFARI, M. R. *et al.* Perspective of Fe3O4 Nanoparticles Role in Biomedical Applications. [*S. l.: s. n.*], v.2016, p. 7840161, 2016.
GILES, A. C.; RANKIN, C. H. Behavioral and genetic characterization of habituation using Caenorhabditis elegans. Neurobiology of Learning and Memory, [*s. l.*], v. 92, n. 2, p. 139-46, 2009.
GONZALEZ-MORAGAS, L.; ROIG, A.; LAROMAINE, A. C. elegans as a tool for in vivo nanoparticle assessment. Advances in Colloid and Interface Science, [*s. l.*], v. 219, p. 10–26, 2015.
HADDAD, P. S. *et al.* Synthesis, characterization, and cytotoxicity of glutathione-PEG-iron oxide magnetic nanoparticles. Journal of Nanoparticle Research, [*s. l.*], v.18, p. 369, 2016.
HARDAKER, L. A. *et al.* Serotonin modulates locomotory behavior and coordinates egg-laying and movement inCaenorhabditis elegans. Journal of Neurobiology, [*s. l.*], v. 49, n. 4, p. 303–313, 2001.
HUNT, P. R. The C. elegans model in toxicity testing. [*S. l.: s. n.*], v. 37, n. 1, p. 50-59, 2017.
HUSSEIN MONTAZERAN, A.; SABER-SAMANDARI, S.; KHANDAN, A. Artificial intelligence investigation of three silicates bioceramics-magnetite bio-nanocomposite: Hyperthermia and

biomedical applications. Nanomed. J, [*s. l.*], v.5, n. 3, p. 163-171, 2018.

JURGONS, R. *et al.* Drug loaded magnetic nanoparticles for cancer therapy. Journal of Physics Condensed Matter, [*s. l.*], v. 18, n. 38, p. S2893, 2006.

KALETTA, T.; HENGARTNER, M. O. Finding function in novel targets: C. elegans as a model organism. [*S. l.: s. n.*], v. 5, n. 5, p. 387-98, 2006.

KIM, S. W.; NAM, S. H.; AN, Y. J. Interaction of Silver Nanoparticles with Biological Surfaces of Caenorhabditis elegans. Ecotoxicology and Environmental Safety, [*s. l.*], v. 77, p. 64-70, 2012.

KINCHEN, J. M. *et al.* Two pathways converge at CED-10 to mediate actin rearrangement and corpse removal in C. elegans. Nature, [*s. l.*], v. 434, n. 7029, p. 93–99, 2005.

KOCH, K. *et al.* Caenorhabditis elegans as model system in pharmacology and toxicology: Effects of flavonoids on redox-sensitive signalling pathways and ageing. [*S. l.: s. n.*], v. 2014, p. 920398, 2014.

KWON, H. J. *et al.* Mitochondria-Targeting Ceria Nanoparticles as Antioxidants for Alzheimeŕs Disease. ACS Nano, [*s. l.*], v. 10, n. 2, p. 2860–2870, 2016.

LUO, X. *et al.* Insights into the Ecotoxicity of Silver Nanoparticles Transferred from Escherichia coli to Caenorhabditis elegans. Scientific Reports, [*s. l.*], v.6, p. 36465, 2016.

MAI, T.; HILT, J. Z. Functionalization of iron oxide nanoparticles with small molecules and the impact on reactive oxygen species generation for potential cancer therapy. Colloids and Surfaces A: Physicochemical and Engineering Aspects, [*s. l.*], v. 576, p. 6-14, 2019.

MARIMON-BOLÍVAR, W. *et al.* Evaluation of the in vivo toxicity of green magnetic nanoparticles using Caenorhabditis elegans as a biological model. Environmental Nanotechnology, Monitoring and Management, [*s. l.*], v. 12, p. 100253, 2019.

MINISTÉRIO DA CIÊNCIA E TECNOLOGIA. Governo do Brasil. Nanotecnologia, 2021. Disponível em <https://antigo.mctic.gov.br/mctic/opencms/tecnologia/tecnologias_convergentes/paginas/nanotecnologia/NANOTECNOLOGIA.html> . Acesso em: 20 de Junho de 2023.

MURPHY, C. T.; HU, P. J. Insulin/insulin-like growth factor signaling in C. elegans. [*S. l.: s. n.*], v. 13, p. 1-43, 2013.

NANOPARTICLES' PROMISES AND RISKS. Characterization, Manipulation, and Potential Hazards to Humanity and the Environment. [*S. l.: s. n.*], v.15, 2015.

OECD. Opportunities and risks of Nanotechnologies. Allianz, [*s. l.*], v. 21, p. 46, 2007.

PIERETTI, J. C. *et al.* Synthesis, Characterization, and Cytotoxicity of Fe3O4@Ag Hybrid Nanoparticles: Promising Applications in Cancer Treatment. Journal of Cluster Science, [*s. l.*], v. 31, n. 2, p. 535–547, 2019.

POON, W. *et al.* Elimination Pathways of Nanoparticles. ACS Nano, [*s. l.*], v. 13, n. 5, p. 5785–5798, 2019.

POSGAI, R. *et al.* Differential toxicity of silver and titanium dioxide nanoparticles on Drosophila melanogaster development, reproductive effort, and viability: Size, coatings and antioxidants matter. Chemosphere, [*s. l.*], v. 85, n. 1, p. 34–42, 2011.

QUEIRÓS, L. *et al.* Caenorhabditis elegans as a tool for environmental risk assessment: emerging and promising applications for a “nobelized worm”. Critical Reviews in Toxicology, [*s. l.*], v. 49, n. 5, p. 411–429, 2019.

RASMUSSEN, K. *et al.* Review of achievements of the OECD Working Party on Manufactured Nanomaterials’ Testing and Assessment Programme. From exploratory testing to test guidelines. Regulatory Toxicology and Pharmacology, [*s. l.*], v. 74, p. 147–160, 2016.

RESHI, M. S. *et al.* Silver nanoparticles protect acetaminophen induced acute hepatotoxicity: A biochemical and histopathological approach. Regulatory Toxicology and Pharmacology, [*s. l.*], v. 90, p. 36–41, 2017.

RINGSTAD, N.; HORVITZ, H. R. FMRFamide neuropeptides and acetylcholine synergistically inhibit egg-laying by C. elegans. Nature Neuroscience, [*s. l.*], v. 11, n. 10, p. 1168–1176, 2008.

RODRIGUES, G. R. *et al.* Antimicrobial magnetic nanoparticles based-therapies for controlling infectious diseases. [*S. l.: s. n.*], v. 555, p. 356-367, 2019.

ROHN, I. *et al.* Selenium species-dependent toxicity, bioavailability and metabolic transformations in: Caenorhabditis elegans. Metallomics, [*s. l.*], v. 10, n. 6, p. 818–827, 2018.

ROLIM, W. R. *et al.* Green tea extract mediated biogenic synthesis of silver nanoparticles: Characterization, cytotoxicity evaluation and antibacterial activity. Applied Surface Science, [*s. l.*], v. 463, p. 66–74, 2019.

SAIFI, M. A.; KHURANA, A.; GODUGU, C. Nanotoxicology: Toxicity and Risk Assessment of Nanomaterials Equal contribution. *In*: NANOMATERIALS IN CHROMATOGRAPHY. [*S. l.: s. n.*], v. 398, n. 2, p. 589-605, 2018.

SALVATI, E.; STELLACCI, F.; KROL, S. Nanosensors for early cancer detection and for

therapeutic drug monitoring. [*S. l.: s. n.*], v. 10, n. 23, p. 3495-512, 2015.

SANVICENS, N.; MARCO, M. P. Multifunctional nanoparticles - properties and prospects for their use in human medicine. [*S. l.: s. n.*], v. 26, n. 8, p. 425-33, 2008.

SCHAFER, W. R. Genetics of Egg-Laying in Worms. Annual Review of Genetics, [*s. l.*], v. 40, n. 1, p. 487–509, 2006.

SEABRA, A. B.; DURÁN, N. Nanotoxicology of metal oxide nanoparticles. [*S. l.: s. n.*], v.5, n.2, p. 934-975, 2015.

SELVARAJ, C. *et al.* Molecular dynamics simulations and applications in computational toxicology and nanotoxicology. Food and Chemical Toxicology, [*s. l.*], v. 112, p. 495-506, 2018.

SUH, W. H. *et al.* Nanotechnology, nanotoxicology, and neuroscience. [*S. l.: s. n.*], v. 87, n. 3, p. 133–170, 2009.

SUN, X.; CHEN, W. D.; WANG, Y. D. DAF-16/FOXO transcription factor in aging and longevity. [*S. l.: s. n.*], v. 8, p. 548, 2017.

TEJEDA-BENITEZ, L.; OLIVERO-VERBEL, J. Caenorhabditis elegans, a biological model for research in toxicology. *In*: REVIEWS OF ENVIRONMENTAL CONTAMINATION AND TOXICOLOGY. [*S. l.: s. n.*], v. 237, p.1-35, 2016.

TESHIBA, E.; MIYAHARA, K.; TAKEYA, H. Glucose-induced abnormal egg-laying rate in *Caenorhabditis elegans*. Bioscience, Biotechnology, and Biochemistry, [*s. l.*], v. 80, n. 7, p. 1436–1439, 2016.

TUNG, L. M. *et al.* Synthesis, characterizations of superparamagnetic Fe3O4-Ag hybrid nanoparticles and their application for highly effective bacteria inactivation. Journal of Nanoscience and Nanotechnology, [*s. l.*], v. 16, n. 6, p. 5902-12, 2016.

WAMUCHO, A.; HEFFLEY, A.; TSYUSKO, O. V. Epigenetic effects induced by silver nanoparticles in Caenorhabditis elegans after multigenerational exposure. Science of the Total Environment, [*s. l.*], v. 725, p. 138523, 2020.

WEINSHENKER, D.; GARRIGA, G.; THOMAS, J. Genetic and pharmacological analysis of neurotransmitters controlling egg laying in C. elegans. The Journal of Neuroscience, [*s. l.*], v. 15, n. 10, p. 6975–6985, 1995.

WOHLFART, S.; GELPERINA, S.; KREUTER, J. Transport of drugs across the blood-brain barrier by nanoparticles. [*S. l.: s. n.*], v. 161, n. 2, p. 264-73, 2012.

WONG, H. L.; WU, X. Y.; BENDAYAN, R. Nanotechnological advances for the delivery of CNS

therapeutics. [*S. l.: s. n.*], v. 64, n. 7, p. 686-700, 2012.

WU, T. *et al.* Caenorhabditis elegans as a complete model organism for biosafety assessments of nanoparticles. [*S. l.: s. n.*], v. 221, p. 708-726, 2019.

YANG, H. H. *et al.* Magnetite-Containing Spherical Silica Nanoparticles for Biocatalysis and Bioseparations. Analytical Chemistry, [*s. l.*], v. 76, n. 5, p. 1316-21, 2004.

YIN, J. *et al.* Time-response characteristic and potential biomarker identification of heavy metal induced toxicity in zebrafish. Fish and Shellfish Immunology, [*s. l.*], v. 72, p. 309–317, 2018.

ZIELIŃSKA, A. *et al.* Nanotoxicology and Nanosafety: Safety-by-Design and Testing at a Glance. International Journal of Environmental Research and Public Health, [*s. l.*], v. 17, n. 13, p. 4657, 2020.